AN EXPERIMENTAL STUDY OF THE VENTILATION OF BLUNT-BASED SURFACE-PIERCING STRUTS

Ray L. Kramer

Lockheed Missiles and Space Company, Incorporated

Prepared for:

Naval Ship Systems Command

November 1972

Final Report

AN EXPERIMENTAL STUDY OF THE VENTILATION OF BLUNT-BASED SURFACE-PIERCING STRUTS

TM 5774-72-19

November 1972 LMSC/D311609

by: R. L. Kramer
Hydrodynamics, 57-74
Ocean Systems
Program Development

Approved: R. L. Waid
R. L. Waid, Manager
Hydrodynamics, 57-74
Ocean Systems
Program Development

This research was sponsored by the
Naval Ships Systems Command
General Hydromechanics Research Program
administered by the
Naval Ship Research and Development Center
Office of Naval Research Contract N00014-72-C-0091

UNCLASSIFIED

Security Classification

DOCUMENT CONTROL DATA - R&D

(Security classification of title, body of abstract and indexing annotation must be entered when the overall report is classified)

1 ORIGINATING ACTIVITY (Corporate author)
LOCKHEED MISSILES & SPACE COMPANY, INC.
A Subsidiary of Lockheed Aircraft Corporation
Sunnyvale, California, 94088

2a REPORT SECURITY CLASSIFICATION
UNCLASSIFIED

2b GROUP

3 REPORT TITLE
AN EXPERIMENTAL STUDY OF THE VENTILATION OF BLUNT-BASED SURFACE-PIERCING STRUTS

4 DESCRIPTIVE NOTES (Type of report and inclusive dates)
Final Report November 1971 - December 1972

5 AUTHOR(S) (Last name, first name, initial)
Ray L. Kramer

6 REPORT DATE	7a TOTAL NO. OF PAGES	7b. NO OF REFS
November 1972	57	6

8a CONTRACT OR GRANT NO.	9a ORIGINATOR'S REPORT NUMBER(S)
N00014-72-C-0091	LMSC/D311609
b. PROJECT NO	TM 5774-72-19
c.	9b. OTHER REPORT NO(S) (Any other numbers that may be assigned this report)
d	

10. AVAILABILITY/LIMITATION NOTICES
Approved for public release; distribution unlimited

11. SUPPLEMENTARY NOTES	12. SPONSORING MILITARY ACTIVITY
	Naval Ship Systems Command General Hydromechanics Research Program

13 ABSTRACT

An experimental program was conducted in the Lockheed Underwater Missile Facility to investigate the ventilation characteristics for surface-piercing blunt-based struts in calm water and in waves. Struts with two leading-edge configurations, one sharp and one blunt, were tested, and the ventilation characteristics are compared with those previously obtained for struts with streamlined trailing edges to determine the effects of the blunt base. The experiments were performed at low ambient pressures to obtain ventilation inception under simultaneous Froude and cavitation number scaled conditions.

Performance comparisons are made at strut yaw angles of six and eight degrees on the bases of resistance to ventilation and of the effects on hydrodynamic forces when ventilation occurs. The blunt-based struts are found to be more subject to ventilation than the streamlined struts. Of the blunt-based struts, ventilation resistance is best for a configuration combining a blunt leading edge with sides contoured to a maximum strut thickness at the base. With respect to hydrodynamic forces, the blunt-based struts are considerably better than the streamlined configurations. The side forces are higher before ventilation and do not decrease as much (and remain in the same direction) after ventilation.

DD FORM 1473

UNCLASSIFIED

Security Classification

14 KEY WORDS	LINK A		LINK B		LINK C	
	ROLE	WT	ROLE	WT	ROLE	WT
Strut						
Ventilation						
Cavitation						
Strut ventilation						
Waves						

TABLE OF CONTENTS

Section	Title	Page
	SUMMARY	i
	TABLE OF CONTENTS	ii
	LIST OF TABLES	iii
	LIST OF FIGURES	iv
	NOMENCLATURE	vi
1.	INTRODUCTION	1
2.	TEST PROGRAM	3
2.1	Model Description	3
2.2	Test Equipment Description	3
2.3	Test Procedures	5
2.4	Data Reduction Procedures	6
3.	RESULTS	8
4.	DISCUSSION OF RESULTS	9
4.1	Ventilation Inception in Calm Water	9
4.1.1	Dependence of cavitation number on Froude number	9
4.1.2	Effect of blunt base	10
4.1.3	Effect of sharp leading edge	11
4.2	Ventilation Inception in Waves	11
4.3	Ventilation Effects on Strut Forces	13
4.4	Mechanism of Ventilation	15
5.	CONCLUSIONS AND RECOMMENDATIONS	17
6.	REFERENCES	19
	TABLES	20
	FIGURES	30

LIST OF TABLES

Table Number	Title	Page
I	Wave Size Combinations	20
II	Ventilation Inception Results Strut Model 2, Blunt-based, 0.76 ft chord, + 6 degrees yaw, Head Seas	21
III	Ventilation Inception Results Strut Model 2, Blunt-based, 0.76 ft chord, + 8 degrees yaw, Head Seas	22
IV	Ventilation Inception Results Strut Model 2, Blunt-based, 0.50 ft chord, + 6 degrees yaw, Head Seas	23
V	Ventilation Inception Results Strut Model 2, Blunt-based, 0.50 ft chord, + 8 degrees yaw, Head Seas	24
VI	Ventilation Inception Results Strut Model 2, Blunt-based, 0.50 ft chord, - 8 degrees yaw, Following Seas	25
VII	Ventilation Inception Results Strut Model 0, Blunt-based, 0.50 ft chord, + 8 degrees yaw, Head Seas	26
VIII	Side Force and Drag Coefficients Blunt-based Strut Model 2, 0.76 ft chord	27
IX	Side Force Coefficients Blunt-based Strut Model 2, 0.50 ft chord	28
X	Side Force and Drag Coefficients Blunt-based Strut Model 0, 0.50 ft chord	29

LIST OF FIGURES

Figure Number	Title
1	Strut model cross sections showing amounts of original streamlined trailing edges removed to form blunt based struts.
2	Photograph of tow carriage with strut model installed.
3	Cavitation number as a function of Froude number at ventilation inception in calm water. Strut model 2, blunt-based, 0.76 ft chord, a 6 and 8 degrees yaw. 1 chord submergence.
4	Cavitation number as a function of Froude number at ventilation inception in calm water. Strut model 2, blunt-based, 0.50 ft chord, at 6 and 8 degrees yaw. 1 chord submergence.
5	Comparison of three trailing-edge variations of strut model 2 with respect to ventilation thresholds in cavitation number as a function of Froude number. 1 chord submergence in calm water.
6	Cavitation number as a function of Froude number at ventilation inception in calm water. Strut model 0, blunt-based, 0.50 ft chord, at 8 degrees yaw. 1 chord submergence.
7	Cavitation number as a function of yaw angle at ventilation inception in calm water for 4.5 Froude number. 1 chord submergence.
8	Effect of head waves on cavitation number at ventilation inception. Strut model 2, blunt-based, 0.76 foot chord, at 6 degrees yaw. 1 chord submergence. Wave length, 14 chords.
9	Effect of head waves on cavitation number at ventilation inception. Strut model 2, blunt-based, 0.76 foot chord, at 8 degrees yaw. 1 chord submergence. Wave length, 14 chords.
10	Effect of head waves on cavitation number at ventilation inception. Strut model 2, blunt-based, 0.50 foot chord, at 6 degrees yaw. 1 chord submergence, Wave length, 14 chords.

LIST OF FIGURES (Concluded)

Figure Number	Title
11	Effect of head and following waves on cavitation number at ventilation inception. Strut model 2, blunt-based, 0.50 foot chord, at 8 degrees yaw. 1 chord submergence. Wave length, 14 chords.
12	Effect of head waves on cavitation number at ventilation inception. Strut model 0, blunt-based, 0.50 foot chord, at 8 degrees yaw. 1 chord submergence. Wave length, 14 chords.
13	Mean cavitation number at ventilation inception as a function of wave height. Head waves, 14 chord wave length. Struts at 8 degrees yaw. Froude number 4.
14	Side force and drag coefficients for blunt-based strut model 2, 0.76 foot chord, at 6 degrees yaw. Submergence 1 chord length.
15	Side force coefficient for blunt-based strut model 2, 0.76 foot chord, at 8 degrees yaw. Submergence 1 chord length.
16	Drag coefficient for blunt-based strut model 2, 0.76 foot chord, at 8 degrees yaw. Submergence 1 chord.
17	Side force coefficient for blunt-based strut model 2, 0.50 foot chord, at 6 degrees yaw. Submergence 1 chord.
18	Side force coefficient for blunt-based strut model 2, 0.50 foot chord, at 8 degrees yaw. Submergence 1 chord.
19	Side force and drag coefficient for blunt-based strut model 0, 0.50 foot chord, at 8 degrees yaw. Submergence 1 chord.
20	Average side force coefficient comparison for blunt-based and streamlined struts, each with sharp and blunt leading edges.
21	Average drag coefficient comparison for blunt-based and streamlined struts, each with sharp and blunt leading edges.

NOMENCLATURE

c		chord of strut model (feet)
A		submerged planform area = c^2 for 1 chord submergence (feet^2)
g	32.15	acceleration of gravity at LUMF (ft/sec^2)
ρ		density of water (slug/ft^3)
V		speed of strut (ft/sec)
F	$V/\sqrt{gc}$	Froude number
P_a		ambient pressure above surface of water (psia)
P_v		vapor pressure of water (psia)
h		wave height (double amplitude) (feet)
λ		wave length (feet)
σ_{vs}	$\frac{(P_a-P_v)\ 144}{\frac{1}{2}\rho V^2}$	surface vapor cavitation number
F_s		side force (pounds)
D		drag (pounds)
C_s	$\frac{F_s}{\frac{1}{2}\rho V^2 A}$	side force coefficient
C_D	$\frac{D}{\frac{1}{2}\rho V^2 A}$	drag coefficient

1. INTRODUCTION

Phenomena associated with the ventilation of surface-piercing struts have been studied by numerous investigators over the last several years. Much of the experimental work has been performed because of the complex interactions of free surface, boundary layer, cavitation, and surface-tension effects on cavitation for which the development of appropriate mathematical models has not been possible. Although the variety of test conditions and configurations used in these studies has been large, they are, unfortunately, in restrictive combinations dictated by the capabilities of the respective test facilities. It is important to note that for full-scale conditions in which ventilation is of potential significance the presence of cavitation can also be expected and adequate consideration for the effects of cavitation must be included.

Development effort aimed at the avoidance of ventilation is usually concentrated on determining the critical shape, arrangement, boundary layer condition, placement of devices (fences), and safe limits of speed and angle of attack. The purpose is to avoid any ventilation, regardless of how it is initiated.

Among the more general investigations of ventilation phenomena have been a number of studies conducted at the Naval Ship Research and Development Center and others supported by the Naval Ship Systems Command General Hydromechancis Research Program administered by the NSRDC.

The General Hydromechanics Research Program has supported four strut-ventilation studies conducted at Lockheed Missiles & Sapce Company, Inc. The fourth of these is the subject of this report. On all four the experimental work has been performed using members of a family of struts designed at NSRDC and tested there also. The parametric variations in this family were leading edge radius and model size.

Studies conducted by investigators at NSRDC[1,2*] in the high-speed towing tank utilizing this family of struts were concerned with the effects of speed and strut geometric parameters on ventilation, cavitation, and other hydrodynamic characteristics. Side-force reversal at ventilation inception was observed and measured. An additional study at NSRDC included waves in the test conditions.

The primary contribution to the program made possible by the tests in the Lockheed Underwater Missile Facility has been the inclusion of cavitation at Froude-scale speeds by virtue of the low ambient pressure capability. Simultaneous cavitation and Froude scaling is accomplished by reducing the ambient pressure above the water surface to small fractions of an atmosphere.

The first study at LMSC[3] was concerned with the mechanism and significant parameters influencing ventilation inception. Leading edge radius was one of the parameters varied. A later study extended this work and included model size as a parametric variation. Forces on the struts before and after ventilation were measured. Yaw angles were small or moderate (4 to 10 degrees) since it was possible to obtain cavitation at small yaw and low speeds. Another study[4] evaluated the effects of waves on ventilation inception.

The objective of the study reported here was to evaluate the ventilation characteristics of blunt-based struts in comparison with streamlined struts. Until now, all of the struts were streamlined with sharp trailing edges. For this study, trailing edges were removed to form two blunt-based configurations with two struts of differing leading edges. Tests were conducted to investigate the conditions leading to ventilation inception in calm water and in waves and to determine the effects of ventilation on hydrodynamic forces on the struts.

---

* Superscripts denote references listed in Section 6.

2. TEST PROGRAM

2.1 Model Description

A family of three blunt-based strut models was obtained by modifying (cutting off the sharp trailing edges) two existing streamlined struts. One of the struts was modified twice so that the three-member family provided (1) two struts with differing leading edge sharpness, one sharp and one blunt, with similar blunt bases in that the sides were parallel at the base, and (2) two struts with the same leading edge (blunt) but differing bases, one boat tailed and one with parallel sides.

The two original streamlined struts were NSRDC model numbers 0 and 2 and had been fabricated for an NSRDC program[1] and also tested on a number of programs at LMSC[3,4] . Ventilation inception characteristics and force coefficients are available from these earlier experiments with the streamlined versions for comparison with the present blunt-based characteristics.

The original struts were of rectangular planform with a 1-foot chord and a span of approximately 4 feet. The lower ends of the struts were square with the span. The maximum strut thickness of 1.44 inches (12 percent of the chord length) was at the mid-chord position, i.e., $\frac{1}{2}$ foot from the leading edge.

The two streamlined and three blunt-based configurations are shown in cross-sectional views in Figure 1. Coordinates for the forward portion of model 2 with the blunt leading edge are available in Reference 3.

2.2 Test Equipment Description

The test program was performed in the Lockheed Underwater Missile Facility utilizing the capability for controlling the ambient pressure above the water surface. Simultaneous cavitation and Froude model scaling are possible in this facility by lowering the ambient pressure to the proper levels. Details of the facility are available in Reference 5. Figure 2 shows the LUMF towing carriage with a strut model installed for testing.

The strut models were attached to a six-component external force balance by an adapter which allowed manual adjustment of the yaw angle of the strut. These tests were conducted with the strut models installed perpendicular to the water surface; i.e., without sweep or dihederal. The force balance was attached to the elevating mechanism which allowed remote adjustment of the depth of submergence of the struts. Both positive and negative yaw angles were used on these tests because the runs were made in both directions, heading into and following the waves. The strut yaw direction (positive means a yaw of the leading edge of the strut to starboard) was selected so that the low pressure side of the strut was always toward the window in which the underwater camera was installed.

The outputs from the force balance were fed to a multi-channel oscillograph which produced oscillograms of the test data. The speed of the towing carriage, the location of the carriage, and a digitally-coded time signal were also recorded on the oscillograms.

Three 16-mm motion picture cameras were utilized to provide optical records of the cavitation on the strut and the ventilation inception. The same digitally-coded time signal was recorded on the film, allowing time-matching with the oscillograms. These cameras were operated at from 80 to 100 frames per second. Two cameras were mounted on the underside of the towing carriage, above water. Each camera viewed slightly downward toward the strut and water surface. One camera was mounted to view the strut from the side and the other was mounted forward viewing approximately 45 degrees aft. The third camera was installed in a viewing port located 2½ feet below the water surface near one end of the towing carriage run - near the termination of the run for following waves and near the beginning of the run for head waves.

The LUMF wave generator was utilized to produce waves of the desired height and wave length. The wave generator consists of a plate, of the dimensions of the end of the water channel, mounted on a shaft driven by a hydraulic pump and cycling mechanism to produce sinusoidal motion. The stroke and cycling frequency were controlled to produce the required waves. A beach

at the opposite end of the water channel absorbs the waves to an extent sufficient to avoid significant wave reflection. A wave height guage in the water channel was used to monitor the waves. The signal from this guage, proportional to instantaneous water surface height, was recorded with the other data on the oscillograms.

2.3 Test Procedures

Test runs with the strut models were performed over a range of test towing speeds, from 14 to 30 ft/sec. The ambient pressure above the water was controlled as the primary test parameter in each series of runs. The pressure was adjusted to provide the conditions necessary for the expected ventilation inception during a run, depending on the strut yaw angle which was set at a fixed amount for the run, on the wave condition, and on the selected towing speed range. The water temperature was measured and recorded daily.

The mean strut submergence was set at one chord length for all tests.

The standard method of acquiring strut speed on each run was to use the catapults to accelerate (1.1 g acceleration) the carriage to a speed approximately 5 ft/sec below the nominal test speed, then use the carriage drive motor to accelerate (0.1 g) to the final speed, after which this speed was maintained until the brake station was reached. The procedure was varied somewhat depending on the length of run desired at constant speed.

On each test day at least one calm water run was made to check the validity of the test data against previous results and to provide an increasing bank of calm water data for comparison with the wave data.

A basic wave size, which was related to the strut chord length, was selected for comparison of wave effects on all struts. The basic wave height was one strut chord length and the wave length was 14 chord lengths. In addition, wave height effects were explored by reducing the height on some of the tests. The wave size combinations used are listed in Table I.

2.4 Data Reduction Procedures

All the data obtained from the external force balance and the three cameras were reviewed and analyzed with regard to the determination of significant parameters controlling ventilation in the presence of cavitation, in both calm water and waves.

The force balance data served to identify the inception of ventilation through a step change in average side force. Any unusual force characteristics were also noted as an aid in assessing the quality and reliability of the test run. The carriage speed at the time of ventilation inception was then read from the oscillogram and the Froude and cavitation numbers were computed. The water vapor pressure needed for the calculation of cavitation number was inferred from the water temperature.

The above-water motion picture records were used as further identification of ventilation inception and were correlated with the force balance records. Ventilation inception is readily identified by a sudden shift in the water surface from a drawn-down sheet covering the cavity to an upward spray position. The underwater-port camera records were reviewed to determine cavitation characteristics and interactions with waves.

The effects of waves on ventilation inception were correlated on the basis of cavitation numbers at ventilation inception. The pressure inside the cavity prior to ventilation was assumed to be the vapor pressure of water, and the ambient pressure was taken at the water surface.

In addition to ventilation inception data, force data were reduced for representative runs in calm water to obtain side force and drag before and after ventilation inception. These were then reduced to coefficient form. The strut acceleration (most of the measurements were read during parts of the runs when the carriage was still being accelerated) was measured for each drag determination and the acceleration force subtracted out to obtain the true drag.

Force records were not reduced for wave tests because of the difficulty of averaging out the oscillatory wave forces over the relatively short intervals of run time before and after ventilation inception.

3. RESULTS

The surface vapor cavitation numbers and the strut Froude numbers at ventilation inception were determined for each test run and are listed in Tables II through VII for each strut configuration, yaw angle, and water surface condition (calm water and waves). A spread in strut speed (Froude number) at ventilation inception was obtained by varying the ambient pressure at the water surface.

The side force and drag were determined for the various strut and yaw angle combinations on representative runs in calm water under both nonventilated and ventilated flow conditions. These values are presented in coefficient form in Tables VIII through X for the three struts. The corresponding surface vapor cavitation numbers are also listed. The cavitation number decreases through the course of a run as the strut speed increases.

The strut characteristics with regard to ventilation inception and force coefficients are compared and discussed in the following section.

4. DISCUSSION OF RESULTS

4.1 Ventilation Inception in Calm Water

4.1.1 Dependence of cavitation number on Froude number

Surface vapor cavitation numbers at ventilation inception were plotted as functions of Froude number. Figures 3 and 4 present those graphs for the blunt leading edge strut, model 2, with the two versions of blunt base. There is also a difference in chord length, and the blunt base configuration is identified in those and subsequent figures by the chord length. The boat-tail version has a chord length of 0.76 feet (Figure 3) and the parallel side version has a chord length of 0.50 feet (Figure 4). Faired curves are drawn through the experimental points to represent the most probable cavitation number threshold for ventilation inception in calm water. Data points for both positive and negative yaws of 8 degrees with the 0.50 foot chord model (Figure 4) did not indicate any difference in the ventilation threshold. Evidently the difference that appeared to exist in the two sides of the streamlined 1.00 foot chord strut (see Reference 4) was removed when the trailing edge was cut off.

The faired curves selected to represent the ventilation thresholds for the two blunt based configurations are compared in Figure 5 together with a curve for the streamlined strut at 8 degrees yaw obtained from the data of Reference 4. This latter curve is the average of the positive and negative 8 degree yaw data. They were averaged in an attempt to remove the apparently asymmetrical effects of the streamlined trailing edge, which are not present in the blunt-base data. In general there is a significant dependence of cavitation number threshold on Froude number with ventilation occurring more readily at higher Froude numbers (and correspondingly higher ambient pressures). Because of the scatter of the data points and the fact that there is not a statistically large sample, the slopes of the curves are considered to be valid as an indication of general trend only. The dependence on Froude number does appear to increase as the yaw angle is increased from 6 degrees to 8 degrees for both blunt-based struts. This was not found to be the case with the streamlined strut.

A similar plot of the ventilation inception data for the sharp leading edge, model 0, blunt-based strut is shown in Figure 6. Only 8 degree yaw data was obtained and, again, the dependence on Froude number appears to be strong. There was no discernable dependence on Froude number for the streamlined version of this strut, although the number of data points available from the previous work is very limited.

4.1.2 Effect of blunt base

It will be noted in Figure 5 that the ventilation inception curves for the streamlined strut at 8 degrees yaw and the 0.76 foot chord boat-tailed strut at 6 degrees yaw are essentially coincident. In other words, the effect of the boat-tail base at 6 degrees yaw is equivalent to increasing the yaw to 8 degrees with the streamlined strut. When the strut is cut off to a 0.50 foot chord with parallel sides at the base, the performance is improved in comparison with the boat-tail base and is approximately the same as for the streamlined strut (both at 8 degrees yaw) in the Froude number range of 4 to 4.5.

A clearer comparison of the effects of the base configuration with respect to yaw can be obtained from Figure 7 in which the average cavitation numbers for ventilation inception are plotted as functions of yaw angle. The average cavitation numbers used are for a Froude number of 4.5 which corresponds to full scale speeds of 48 and 68 knots respectively for 10 feet and 20 feet chord struts. The values for the streamlined strut model 2 were obtained from the data of Reference 4 by estimating the averages for positive and negative yaw angles.

With the blunt leading edge model 2, resistance to ventilation is best for the streamlined strut and worst for the boat-tailed strut, with the parallel-sided blunt-based strut results falling between. The parallel-sided strut does not appear to be as adversely affected by increasing the yaw angle from 6 to 8 degrees as either of the others, whereas the boat-tailed strut is most strongly affected.

The effect of the blunt base (parallel sides) on the sharp leading edge model 0 is very large, the cavitation number at ventilation inception being nearly 3 times that for the streamlined base at the only yaw angle (8 degrees) investigated. This is in sharp contrast to the almost negligible effect of the parallel sided blunt base on ventilation at 8 degrees yaw for model 2.

4.1.3 Effect of sharp leading edge

The effect of the leading edge sharpness on ventilation inception trends cannot be very clearly defined from the data available here except in relation to other factors such as trailing edge sharpness or the presence of waves. Originally it was planned to test a model with leading edge sharpness between that of models 0 and 2 but this model was unavailable and the plan was changed. The observations are limited, therefore, to the facts that for a streamlined base in calm water (at 8 degrees yaw) the sharp leading edge provides slightly better resistance to ventilation than the blunt leading edge, but for a blunt-based strut the sharp leading edge is much worse than the blunt leading edge. In the latter case ventilation occurs at about twice the cavitation number for the blunt leading edge.

4.2 Ventilation Inception in Waves

The cavitation numbers at ventilation inception in waves are plotted as functions of Froude number in Figures 8 through 12. The calm water average ventilation thresholds are included for comparison.

The principal wave size used to compare wave effects on all struts was the largest deemed reasonable for a strut submergence of one chord. This large wave was selected to emphasize the effect on ventilation and make it easily discernable in all cases. On this wave, of one chord wave height, the strut submergence at the wave trough was only one-half chord. For some strut and yaw angle conditions waves one-half and one-fourth as high were also used to determine ventilation variation with wave height. The wave length for all these was 14 chords, selected on the basis that for the highest wave the height/length ratio would be one-half the limit of 1:7 near which the wave

breaks. No clear indication was observed from the motion pictures or force balance data that a different mechanism of ventilation was triggered by the shallow strut submergence at the trough of the highest wave. However, ventilation inception did occur frequently in or near the trough , on all wave heights, in head waves with the blunt-based struts. This was not the case in the earlier work with streamlined struts in head waves where ventilation inception almost invariable occurred at or near the wave crest. The same relative range of wave heights (up to one chord) was used with those struts.

The wave ventilation data scatter is larger with the maximum wave than with smaller waves, at least for the boat-tail (blunt leading edge) and the sharp leading edge struts; see Figures 9 and 12.

In following waves, the effect on ventilation is considerably smaller than for head waves of the same size; see Figure 11. This difference was also observed for the streamlined strut[4].

Ventilation inception cavitation numbers are plotted as a function of wave height, Figure 13, for the three blunt-based struts at an eight degree yaw in head waves. Curves are included which predict the wave effects on the basis of water particle orbital speed being added to the strut speed at the wave crest to obtain the maximum local relative speed. Increasing mean cavitation numbers (based on mean, or strut, speed) are predicted as wave height increases since ventilation should occur at lower strut speeds. The orbital speeds were obtained using a non-linear theory[6] based on gravity waves with a profile represented by a Fourier series to the third order. The wave effect prediction curves were fitted to the calm water ventilation cavitation numbers at a Froude number of four which appear on the graph of Figure 13 at zero wave height. The actual wave data were adjusted to a Froude number of four by projecting the data points nearest that Froude number along a line parallel to the calm water line (Figures 9, 11, 12).

It is seen that all the wave ventilation data points lie at higher cavitation numbers than predicted on the basis of orbital speeds, including those for the lowest, one-fourth chord, wave heights, and that the amount of the difference

remains approximately constant for all wave heights. One exception exists, Figure 8, for the half chord wave heights with the boat-tail strut at six degrees yaw.

The strut with the smallest wave effect appears to be the blunt-leading edge, model 2, with the parallel side blunt base, 0.50 foot chord. This is also the strut that is most resistant to ventilation in calm water.

4.3 Ventilation Effects on Strut Forces

The side force and drag coefficients for the three blunt-based strut models in calm water are presented in Figures 14 through 19. In these figures the forces measured under non-ventilated conditions are represented by an open symbol and the forces measured under ventilated conditions are represented by a solid symbol. The side force and drag changed quickly at ventilation inception and generally remained stable afterward. With the boat-tailed model 2, 0.76 foot chord, it was noted on some runs, however, that the drag suddenly increased a considerable amount after an interval of 0.6 to 1 second following ventilation inception, see Figures 14 and 16. The side force did not change at that time. Since the time at which the jump in drag occurred was near the end of the run, it may have been missed in other cases because of the termination of the run. The motion pictures were inspected for clues of changes in flow appearance that might be associated with the jump in drag and none could be found. No explanation could be found that might indicate the apparent drag increase was spurious, although this possibility cannot be entirely ruled out.

Unfortunately no drag data are available for the strut model 2, 0.50 foot chord length because toward the end of the test program (this model was tested last) the force balance drag cell became inoperative and could not be repaired in time.

Both positive and negative yaw force data ($\pm$ 8 degrees) were included in Figure 18 since no difference was found in magnitude (the sign of the -8 degree data was reversed for the purposes of this plot).

The side forces decrease markedly at ventilation inception and remain low in the ventilated condition for the blunt-based struts but they do not reverse to the opposite direction as they did for the streamlined struts[3]. The larger effects of ventilation on side force for the streamlined struts is what one would expect since the wall pressure on the "high pressure" side of the trailing edge portion of the strut is low. When this strut is ventilated a large area of the aft portion is subject to the ambient pressure in the cavity with resulting forces in the opposite direction. Some of this effect apparently remains for the 0.76 foot chord blunt-based strut at six degrees yaw because not enough of the aft portion was cut away. When the strut was cut to 0.50 foot chord length the side force change at ventilation was much reduced.

The effects of ventilation on side force are summarized for the blunt-based and streamlined struts in Figure 20. The improved performance of the blunt-based struts with respect to side force can be seen for the six and eight degrees yaw angles tested. Of the two blunt leading edge models (model 2) tested, the more blunt-based (0.50 foot chord) has better characteristics at six degrees yaw but the two are essentially the same at eight degrees yaw. Perhaps the most marked improvement in blunt-based over streamlined configuration occurs with the sharp-leading-edge model 0. Here the side force coefficient for the non-ventilated blunt based strut is more than twice the value for the streamlined strut, and in the ventilated condition the blunt-based strut side force coefficient is essentially the same as that for the streamlined strut when it was not ventilated.

The possible over-all advantages of the blunt-based, 0.50 foot chord, model 2 strut over the streamlined strut can be illustrated by comparing the performance for a given side force. If a side force coefficient of .185 is said to be required for a certain craft operating condition, this can be achieved with the blunt-based strut at a yaw angle of 6 degrees (Figure 20) whereas a yaw of 9 degrees is necessary with the streamlined strut (both non-ventilated). If ventilation should occur, the side force coefficient drops to .095 for the blunt based strut but it reverses, to -.085, for the streamlined strut. Furthermore, at these two yaw angles of 6 and 9 degrees,

respectively, the blunt-based strut is less likely to ventilate than the streamlined strut (See Figure 7).

A price appears to be paid in terms of increased drag, Figure 21, for the blunt-based model 0 strut over that for the streamlined strut. With the model 2 strut, the 0.76 foot chord blunt-based version has slightly reduced drag, compared with the streamlined version at six degrees yaw but at eight degrees, in the ventilated condition, the blunt based drag is greater. The possibility of greatly increased drag, delayed after ventilation inception remains for the blunt-based strut, especially at eight degrees yaw. As stated earlier, no drag data were obtained for the model 2 blunt-based 0.50 foot chord strut.

4.4 Mechanism of Ventilation

The break through to the low pressure vapor-filled side cavity, which allows ambient air to blow in at ventilation inception, most probably occurs near the base of the blunt-based strut when the vapor-filled cavity grows sufficiently in length to come in close proximity to the base cavity. This base cavity is open at the surface and can provide a passageway for air to flow into the side cavity. Although the base cavity can be seen in the motion pictures taken from both above and below the water surface, no clues were obtained from the pictures to indicate the exact mechanism of the ventilation inception. The above-water pictures show clearly the surface flow features of base cavity and the change in the angle of the surface near the strut leading edge (resulting in spray) when ventilation occurs. They also show indistinct shadow-like outlines of the below-surface vapor cavity before ventilation and some idea of the approximate size and extent of this cavity was obtained. The underwater camera was at a fixed lacation in a tank window and no ventilation inception events occurred in good view of this camera.

Since ventilation occurs when the side cavity is of the approximate size to bring it close to the base cavity and since ventilation occurs more readily (at higher cavitation numbers) with the blunt-based struts than with streamlined struts, it appears that the ventilation occurs through the wall of the base cavity.

It was noted that at eight degrees yaw the dependence of cavitation number at ventilation inception on Froude number was much stronger (see Figures 5 and 6) for the blunt-based struts than for the streamlined ones. The dependence is approximately a first power (of Froude number) one rather than a 0.2 power as found for the streamlined struts which may indicate that the significant depth for ventilation is farther below the water surface.

5. CONCLUSIONS AND RECOMMENDATIONS

The following conclusions have been drawn from this study of the ventilation of blunt-based struts.

Ventilation Inception

1. Blunt-based struts are not as resistant to ventilation as are streamlined struts.

2. Greater susceptibility to ventilation is probably associated with the proximity of the ventilated base cavity to the side vapor cavity of the blunt-based strut and the ease with which the air can break through from the base cavity into the vapor cavity.

3. Of the two blunt-based struts with the same blunt leading edge the one with the maximum thickness at the base is more resistant to ventilation than is the one with a boat tail.

4. Much greater susceptibility to ventilation resulted from making the sharp-leading-edge strut blunt-based than from making the same variation with the blunt-leading-edge strut.

5. The presence of head waves caused ventilation to occur more readily than in calm water. The effect of the waves was greater than would be predicted on the basis of increased relative velocity due to wave orbital velocity at the wave crest.

6. The effect of following waves is less than head waves.

7. The effect of waves was the least for the blunt-leading-edge, blunt-based strut with maximum thickness at the base.

Side Force and Drag

1. The blunt-based struts were found to have higher side force coefficients (both ventilated and nonventilated) than the corresponding streamlined struts.

2. Side force differences associated with ventilated as compared with nonventilated flow conditions were less for the blunt-based struts than for the streamlined struts.

3. In the case of the sharp-leading-edge strut, the side force coefficient for the ventilated blunt-based configuration was found to be as large as for the nonventilated streamlined configuration.

4. The drag of the sharp-leading-edge strut at an eight degree yaw angle was increased considerably by giving it a blunt base.

5. Anomalous increases in drag were found for the boat-tailed blunt-leading-edge strut at a time of 0.6 to 2.0 second after ventilation inception.

RECOMMENDATIONS

1. The effects of the degree of leading-edge sharpness on ventilation and forces should be investigated more fully with struts of intermediate sharpness.

2. The sharp-leading-edge blunt-based strut should be considered further, in view of its high side force coefficient, both nonventilated and ventilated, even though it is highly susceptible to ventilation. The strut might be operated at smaller yaw angles to avoid ventilation or it might be operated ventilated (with forced ventilation to avoid uncontrolled side force changes) provided the drag is acceptable. The side force, drag, and ventilation characteristics should be investigated at angles of yaw smaller than eight degrees.

3. Investigations should be made of the force characteristics of blunt-based struts combined with flaps operating on the walls of the base cavity.

4. Investigation should be made of the amount of strut drag at a time considerably later than the occurrence of ventilation to clear up the anomaly observed in this study.

6. REFERENCES

1. Rothblum, R. S., and Wilburn, G. M., "Investigation of Ventilation of Surface Piercing Struts", Naval Ship Research and Development Center, Test and Evaluation Report 217-H-01, June 1967.

2. Rothblum, R. S., Mayer, D. A., and Wilburn, G. M., "Ventilation, Cavitation and Other Characteristics of High Speed Surface-Piercing Struts", Naval Ship Research and Development Center, Hydromechanics Laboratory Research and Development Report 3023, July 1969.

3. Waid, R. L., "Experimental Investigation of the Ventilation of Vertical Surface Piercing Struts in the Presence of Cavitation", Lockheed Missiles & Space Company, Report Number LMSC/D019597, May 1968.

4. Kramer, R. L., "An Experimental Study of the Effects of Waves on the Ventilation of Surface-Piercing Struts", Lockheed Missiles & Space Co., Report Number LMSC/D029678, November, 1970.

5. Waid, R. L., "Cavitation Research Capabilities of the Lockheed Underwater Missile Facility", Symposium on Cavitation Research Facilities and Techniques, American Society of Mechanical Engineers, 1964.

6. Wehausen, John V., and Laitone, Edmunds V., "Surface Waves", Handbuch der Physik, Volume IX.

TABLE I

WAVE SIZE COMBINATIONS

Blunt-Based Strut Model	Wave Height, Length (feet)	(chord lengths)	Reciprocal of Wave steepness Length/Height
"2", 0.76 ft chord	3/4, 10.5	1 , 14	14
	1/2, 7	2/3, 9.3	14
	3/8, 10.5	1/2, 14	28
	3/16, 10.5	1/4, 14	56
"2", 0.50 ft chord	1/2, 7	1 , 14	14
"0", 0.50 ft chord	1/2, 7	1 , 14	14
	1/4, 7	1/2, 14	28

TABLE II

VENTILATION INCEPTION RESULTS

Strut Model 2, Blunt-based, 0.76 ft chord,
+6 degrees yaw, Head Seas

Waves Height x Length (Chord Lengths)	Run No.	Strut Speed (ft/sec)	Froude Number	$P_a - P_v$ (psi)	Cavitation Number
Calm Water	12	20.6	4.15	.685	.243
	13	18.6	3.74	.477	.209
	16	27.8	5.64	1.32	.254
	18	27.0	5.45	1.22	.252
	24	23.2	4.68	.850	.238
	25	22.1	4.46	.529	.246
1/2 x 14	83	15.9	3.21	.374	.223
	84	16.9	3.41	.358	.187
	86	19.4	3.90	.565	.225
	87	20.4	4.11	.772	.209
	89	23.7	4.77	1.06	.281
	91	23.1	4.66	1.00	.281
2/3 x 9.3	33	16.7	3.36	.462	.246
	35	25.0	5.04	1.20	.285
	36	24.1	4.85	1.15	.295
	38	25.5	5.15	1.22	.278
1 x 14	92	20.4	4.11	1.00	.360
	93	20.8	4.20	.972	.343
	95	17.8	3.60	.652	.309
	97	17.1	3.45	.628	.324

TABLE III

VENTILATION INCEPTION RESULTS

Strut Model 2, Blunt-based, 0.76 ft chord,

+8 degrees yaw, Head Seas

Waves Height x Length (Chord Lengths)	Run No.	Strut Speed (ft/sec)	Froude Number	$P_a - P_v$ (psi)	Cavitation Number
Calm Water	41	22.0	4.44	1.20	.370
	42	15.8	3.19	.474	.282
	43	15.4	3.11	.410	.255
	44	14.1	2.84	.360	.279
	45	14.7	2.96	.344	.237
	46	17.3	3.48	.698	.347
	50	23.2	4.68	1.63	.437
	51	23.6	4.77	1.60	.424
	52	23.1	4.66	1.56	.434
	53	22.8	4.51	1.49	.424
1/4 x 14	73	20.4	4.11	1.28	.469
	74	19.7	3.97	1.26	.482
	75	19.7	3.97	1.26	.482
	76	18.4	3.71	.834	.367
	77	16.0	3.23	.594	.343
	78	15.2	3.06	.569	.367
	79	14.3	2.88	.466	.340
1/2 x 14	66	18.8	3.79	1.06	.447
	67	17.8	3.60	1.02	.474
	68	15.1	3.05	.599	.388
	69	15.4	3.11	.643	.403
	70	18.5	3.73	1.14	.495
	71	20.0	4.03	1.26	.472
	72	19.5	3.93	1.25	.490
1 x 14	54	20.8	4.19	1.53	.527
	55	21.2	4.27	1.59	.526
	56	19.8	3.99	1.56	.591
	57	19.3	3.89	1.58	.630
	58	20.6	4.15	1.68	.589
	59	21.6	4.35	1.69	.538
	61	17.4	3.51	1.56	.767
	63	14.3	2.90	.566	.440
	65	13.2	2.67	.501	.423

TABLE IV

VENTILATION INCEPTION RESULTS

Strut Model 2, Blunt-based, 0.50 ft chord,
+6 degrees yaw, Head Seas

Waves Height x Length (Chord Lengths)	Run No.	Strut Speed (ft/sec)	Froude Number	$P_a - P_v$ (psi)	Cavitation Number
Calm Water	154	21.3	5.32	.667	.218
	155	19.7	4.90	.589	.226
	156	18.8	4.70	.535	.224
	157	17.8	4.43	.456	.214
	158	15.8	3.96	.388	.230
	164	22.1	5.50	.707	.215
	167	19.7	4.91	.574	.220
	168	28.6	7.12	1.21	.220
1 x 14	159	15.5	3.87	.343	.213
	160	15.9	3.96	.422	.248
	161	18.5	4.62	.570	.248
	162	20.3	5.06	.712	.257
	163	21.8	5.43	.834	.261
	166	18.1	4.51	.623	.283

TABLE V

VENTILATION INCEPTION RESULTS

Strut Model 2, Blunt-based, 0.50 ft chord,
+8 degrees yaw, Head Seas

Waves Height x Length (Chord Lengths)	Run No.	Strut Speed (ft/sec)	Froude Number	$P_a - P_v$ (psi)	Cavitation Number
Calm Water	133	22.9	5.72	1.08	.307
	135	19.6	4.88	.805	.312
	137	19.9	4.98	.775	.291
	138	20.6	5.13	.722	.253
	139	20.1	5.01	.731	.269
	140	19.2	4.79	.624	.251
	151	18.5	4.62	.559	.242
	152	17.2	4.29	.476	.243
1 x 14	141	21.2	5.30	1.05	.359
	142	21.2	5.28	.923	.305
	144	19.8	4.94	.800	.304
	145	18.0	4.48	.750	.344
	146	19.5	4.86	.849	.337
	147	21.1	5.25	.942	.305
	148	19.4	4.85	.868	.342
	149	18.8	4.70	.756	.317
	150	16.8	4.18	.633	.333

TABLE VI

VENTILATION INCEPTION RESULTS

Strut Model 2, Blunt-based, 0.50 ft chord,
-8 degrees yaw, Following Seas

Waves Height x Length (Chord Lengths)	Run No.	Strut Speed (ft/sec)	Froude Number	$P_a - P_v$ (psi)	Cavitation Number
Calm Water	170	19.8	4.93	.667	.254
	171	18.7	4.66	.594	.252
	172	17.1	4.26	.471	.240
	174	16.5	4.11	.422	.231
	179	19.6	4.90	.677	.261
	180	20.8	5.18	.815	.280
	182	21.4	5.33	.923	.300
	183	22.7	5.66	1.07	.309
1 x 14	175	16.7	4.17	.471	.250
	176	16.5	4.11	.481	.263
	177	17.5	4.37	.579	.279
	178	19.3	4.82	.692	.276
	181	20.6	5.13	.815	.285

TABLE VII

VENTILATION INCEPTION RESULTS

Strut Model O, Blunt-based, 0.50 ft chord,

+8 degrees yaw, Head Seas

Waves Height x Length (Chord Lengths)	Run No.	Strut Speed (ft/sec)	Froude Number	$P_a - P_v$ (psi)	Cavitation Number
Calm Water	100	15.2	3.78	.702	.452
	103	14.7	3.67	.697	.480
	104	14.8	3.69	.697	.473
	105	14.8	3.69	.707	.480
	107	19.6	4.88	1.60	.622
	108	19.7	4.92	1.67	.636
	109	19.8	4.95	1.75	.660
	116	20.6	5.13	1.78	.622
	119	18.6	4.64	1.18	.506
	128	17.5	4.36	1.20	.584
1/2 x 14	110	19.8	4.94	2.03	.769
	114	19.7	4.92	1.93	.741
	115	19.6	4.88	2.00	.775
	117	16.1	4.01	1.16	.667
	118	16.5	4.11	1.20	.656
1 x 14	120	20.1	5.02	1.93	.707
	121	19.2	4.79	1.97	.795
	122	18.6	4.64	2.09	.900
	123	19.1	4.76	2.26	.920
	124	20.0	4.98	2.44	.907
	125	16.3	4.06	1.36	.761
	126	16.3	4.06	1.44	.805
	127	17.4	4.34	1.45	.712
	129	20.4	5.08	1.98	.708

TABLE VIII

SIDE FORCE AND DRAG COEFFICIENTS

Blunt-based Strut Model 2, 0.76 ft. chord

Run No.	Nonventilated Cavitation No.	Nonventilated Sideforce Coeff.	Nonventilated Drag Coeff.	Ventilated Cavitation No.	Ventilated Sideforce Coeff.	Ventilated Drag Coeff.
6 degrees yaw						
12	.267	.216	.095	.241	-.011	.030
13	.227	.212	.078	.194	-.007	.032
16	.258	.178	.047	.242	+.016	.012
				.219*		.108*
18	.251	.146	.057	.237	-.015	.065
				.203*		.154*
24	.249	.147	.078	.223	-.014	.051
25	.212	.216	.046	.152	.000	.053
8 degrees yaw						
41	.381	.178	.011	.347	.018	.073
				.288*		.791*
42	.295	.292	.125	.261	.049	.102
43	.266	.297	.108	.228	.077	.060
44	.283	.312	.154	.241	.123	.053
				.128*		.765*
45	.261	.270	.065	.219	.102	.018
46	.355	.180		.385	.062	
50	.462	.227	.080	.414	.037	.154
				.391*		.838*
51	.444	.233	.075	.380	.021	.061
				.360*		.484*
52	.477	.251	.076	.415	.048	.058
				.377*		.69 *
53	.441	.239	.080	.392	.048	.098
				.355*		.705*

* Abrupt increase in drag occurring after an interval of 0.6 to 1 second after ventilation inception.

TABLE IX

SIDE FORCE COEFFICIENTS

Blunt-based Strut Model 2, 0.50 ft. chord

Run Number	Nonventilated		Ventilated	
	Cavitation Number	Sideforce Coefficient	Cavitation Number	Sideforce Coefficient
6 degrees yaw				
154	.225	.194	.204	.104
155	.241	.198	.211	.084
167	.234	.160	.208	.095
8 degrees yaw				
135	.328	.254	.293	.068
137	.307	.292	.276	.064
139	.283	.285	.252	.036
152	.264	.279	.228	.073
-8 degrees yaw				
170	.271	-.281	.236	-.054
179	.272	-.207	.243	-.028
180	.286	-.240	.268	-.026

TABLE X

SIDE FORCE AND DRAG COEFFICIENTS

Blunt-based Strut Model 0, 0.50 ft. chord

Run No.	Nonventilated			Ventilated		
	Cavitation No.	Sideforce Coeff.	Drag Coeff.	Cavitation No.	Sideforce Coeff.	Drag Coeff.
8 degrees yaw						
100	.476	.401	.115	.417	.119	.121
103	.521	.298	.193	.438	.115	.118
104	.518	.313	.147	.436	.146	.164
105	.527	.249	.197	.449	.072	.125
107	.645	.177	.159	.607	.089	.138
108	.680	.189	.094	.620	.022	.086
109	.692	.476	.131	.619	.241	.081
116	.674	.311	.063	.599	.165	.056
119	.547	.268		.485	.130	
128	.623	.274		.540	.174	

MODEL 0

Circular arc contour (radius 25.36 in)
Sharp leading edge included angle, 27.2 deg
Maximum thickness, 1.44 in, at original midchord

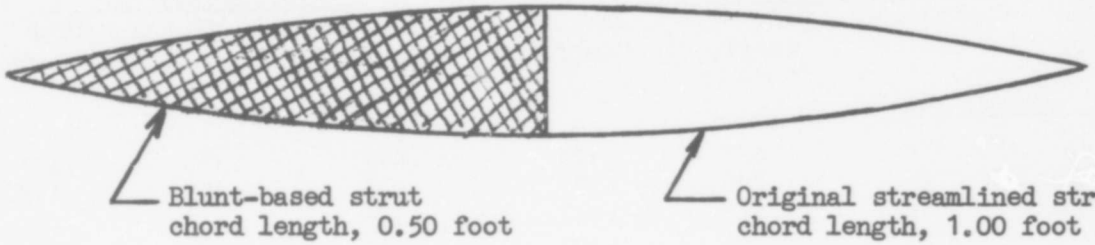

MODEL 2

Circular arc contour (radius 25.36 in) from midchord
to original trailing edge. Leading edge radius, 0.219 in.
Maximum thickness, 1.44 in, at original midchord

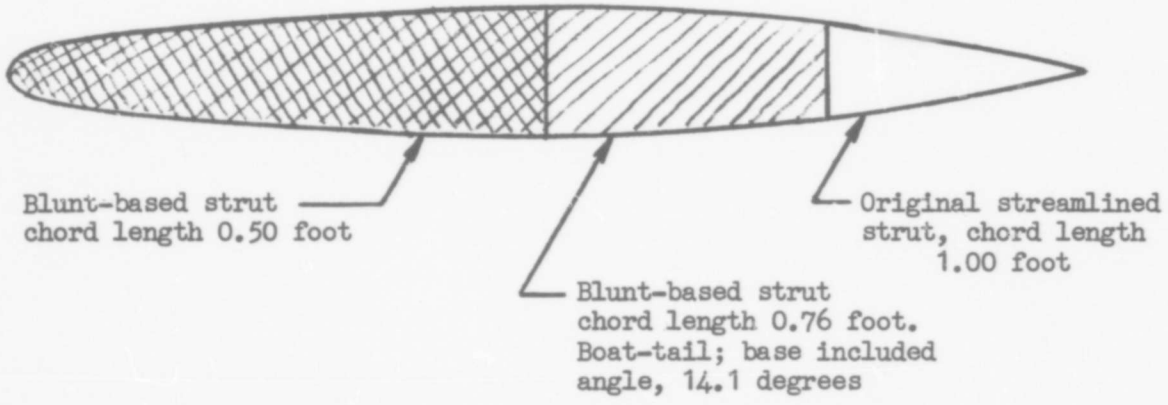

Fig. 1 Strut model cross sections showing amounts of original streamlined trailing edges removed to form blunt based struts.

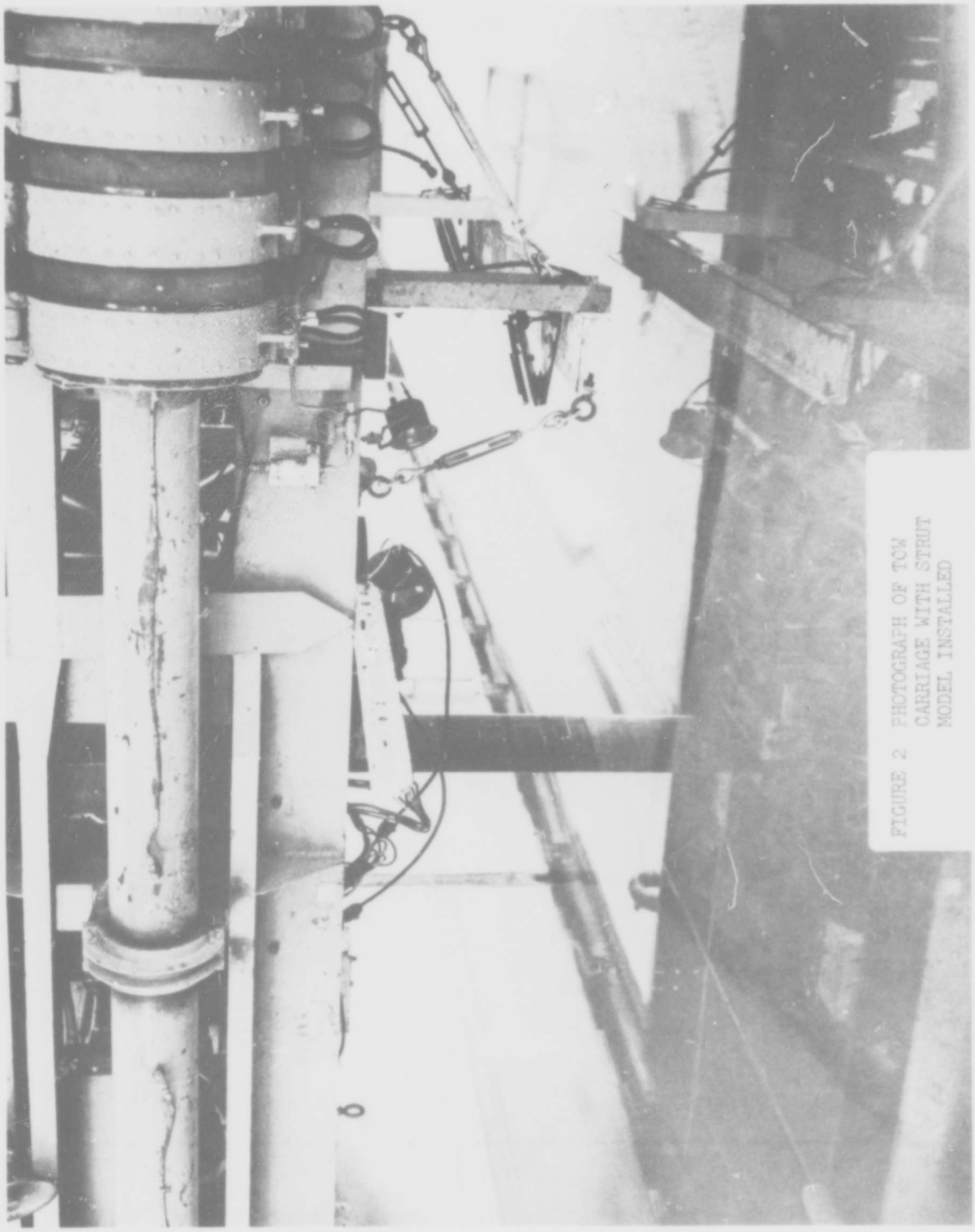

FIGURE 2 PHOTOGRAPH OF TCW CARRIAGE WITH STRUT MODEL INSTALLED

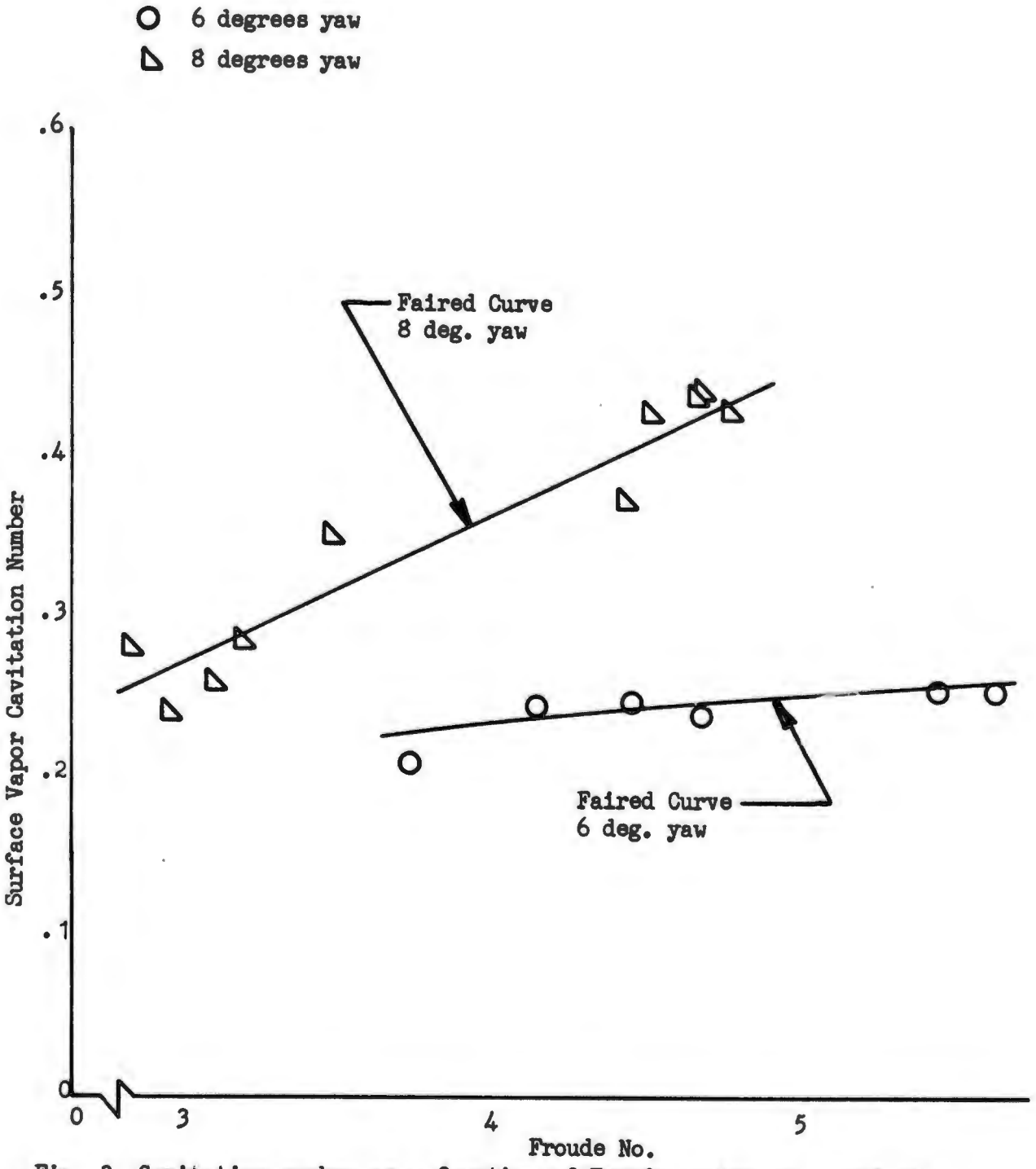

Fig. 3 Cavitation number as a function of Froude number at ventilation inception in calm water. Strut model 2, blunt-based, 0.76 ft chord, at 6 and 8 degrees yaw. 1 chord submergance.

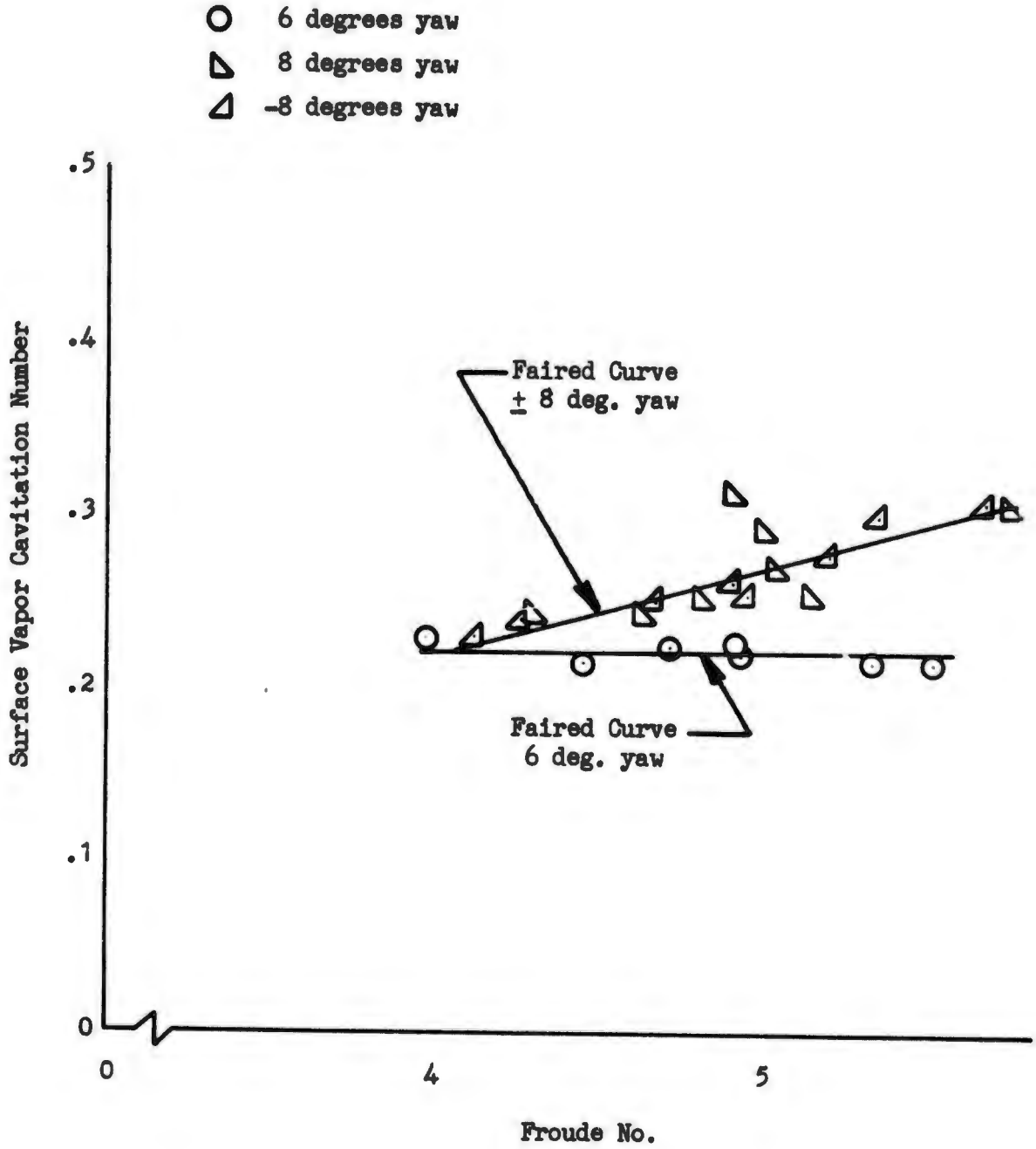

Fig. 4 Cavitation number as a function of Froude number at ventilation inception in calm water. Strut model 2, blunt-based, 0.50 foot chord, at 6 and 8 degrees yaw. 1 chord submergence.

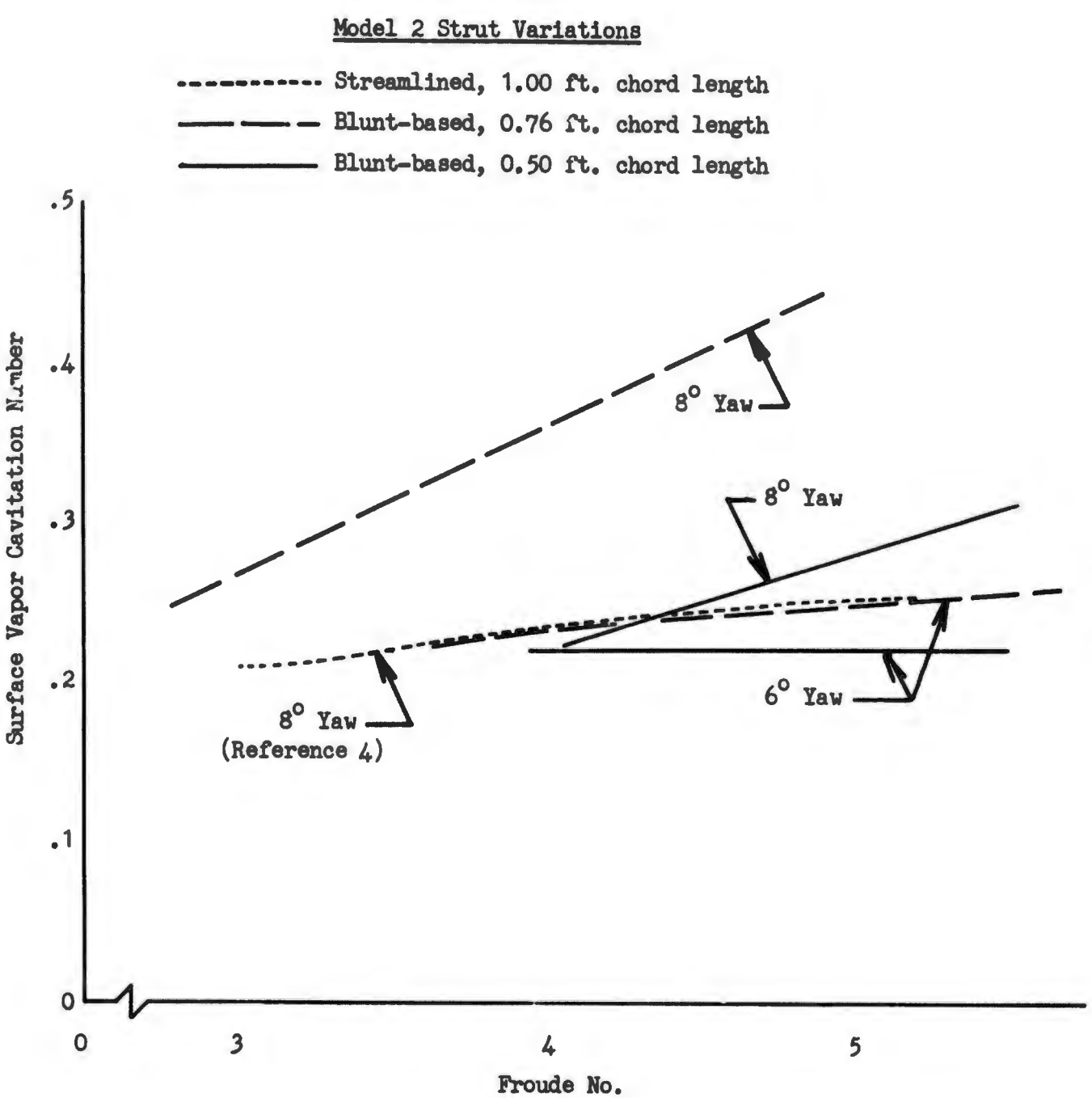

Fig. 5 Comparison of three trailing-edge variations of strut model 2 with respect to ventilation thresholds in cavitation number as a function of Froude number. 1 chord submergence in calm water.

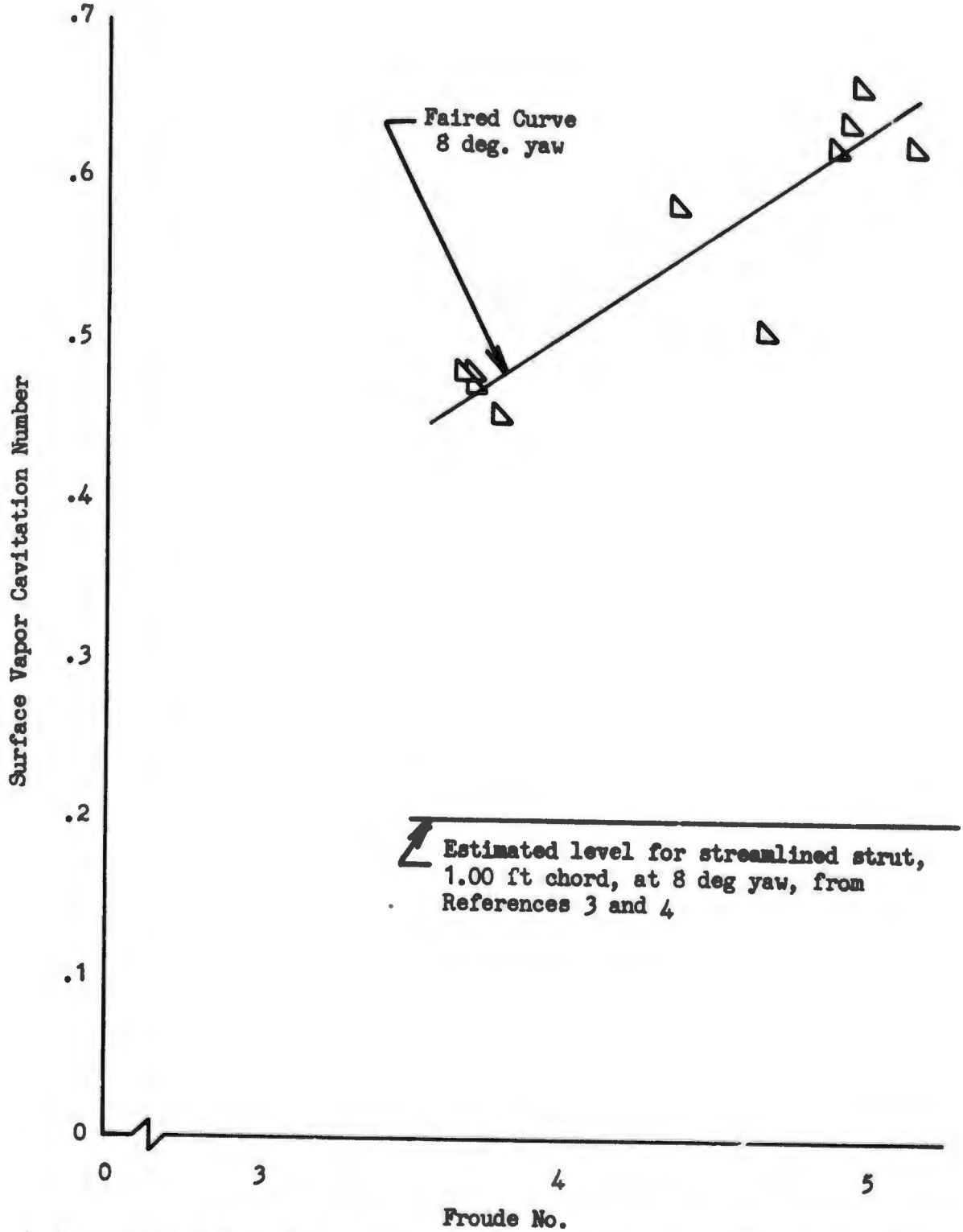

Fig. 6 Cavitation number as a function of Froude number at ventilation inception in calm water. Strut model 0, blunt-based, 0.50 foot, chord, at 8 degrees yaw. 1 chord submergence.

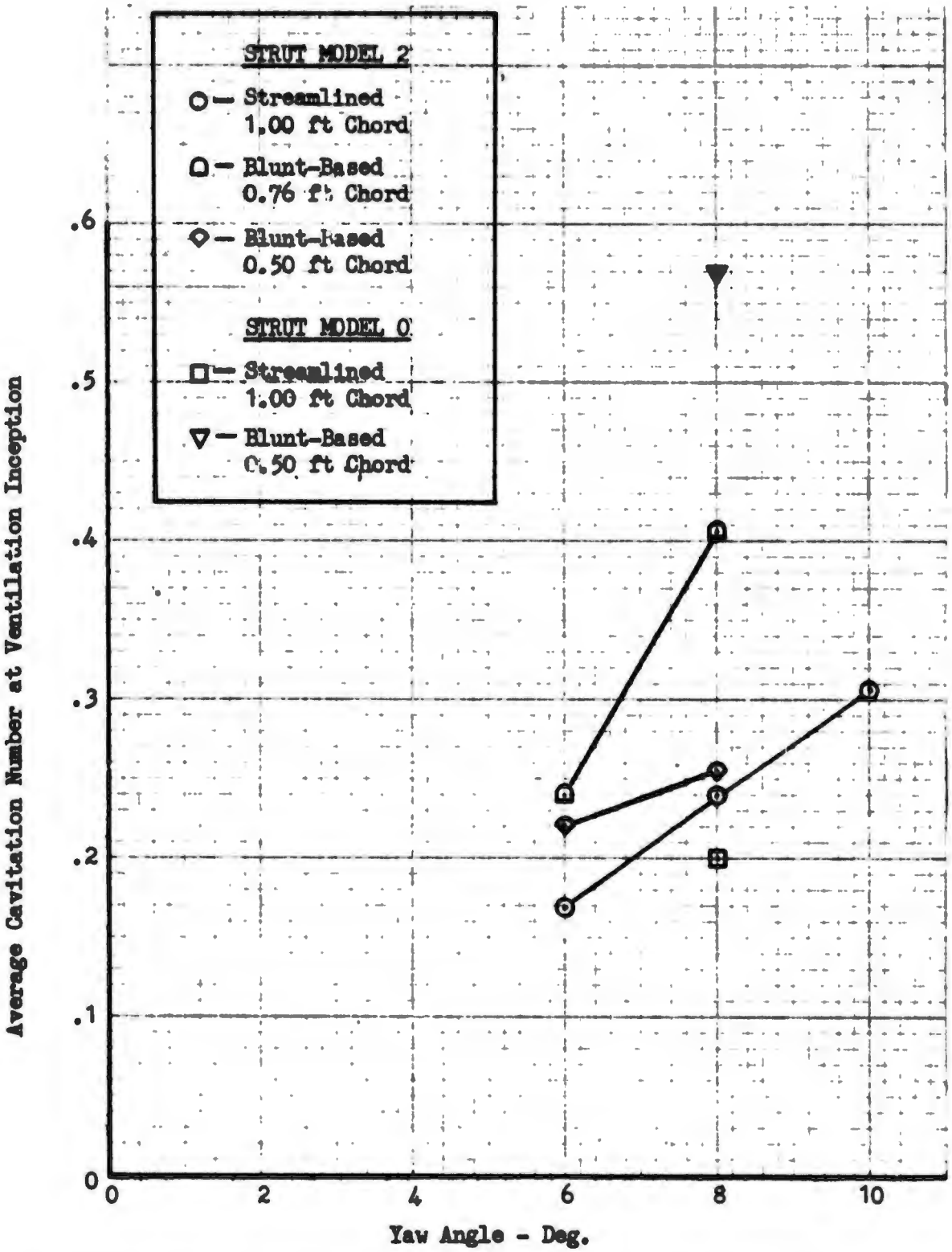

Fig. 7 Cavitation number as a function of yaw angle at ventilation inception in calm water for 4.5 Froude number. 1 chord submergence.

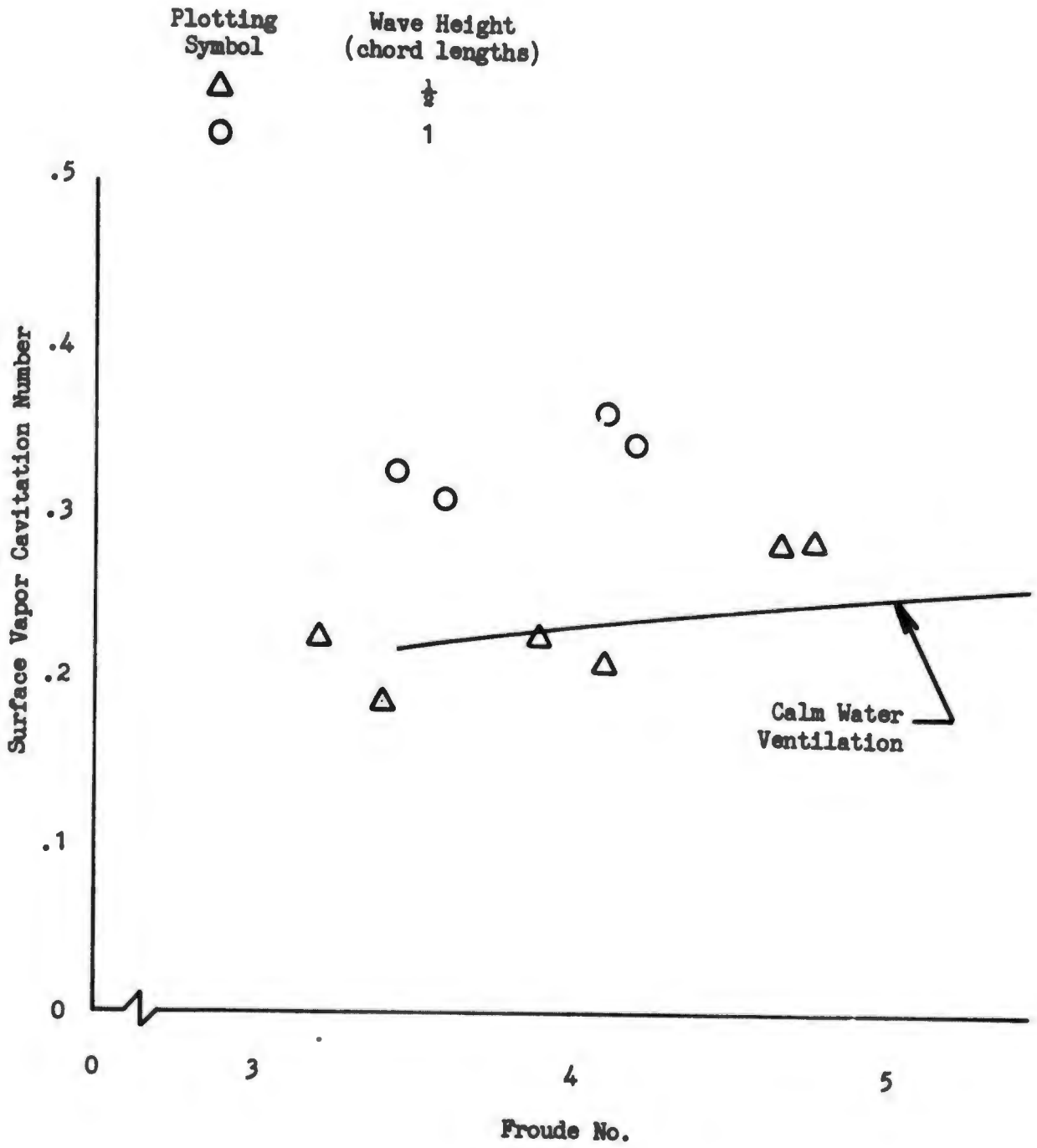

Fig. 8 Effect of head waves on cavitation number at ventilation inception. Strut model 2, blunt-based, 0.76 foot chord, at 6 degrees yaw. 1 chord submergence. Wave length, 14 chords.

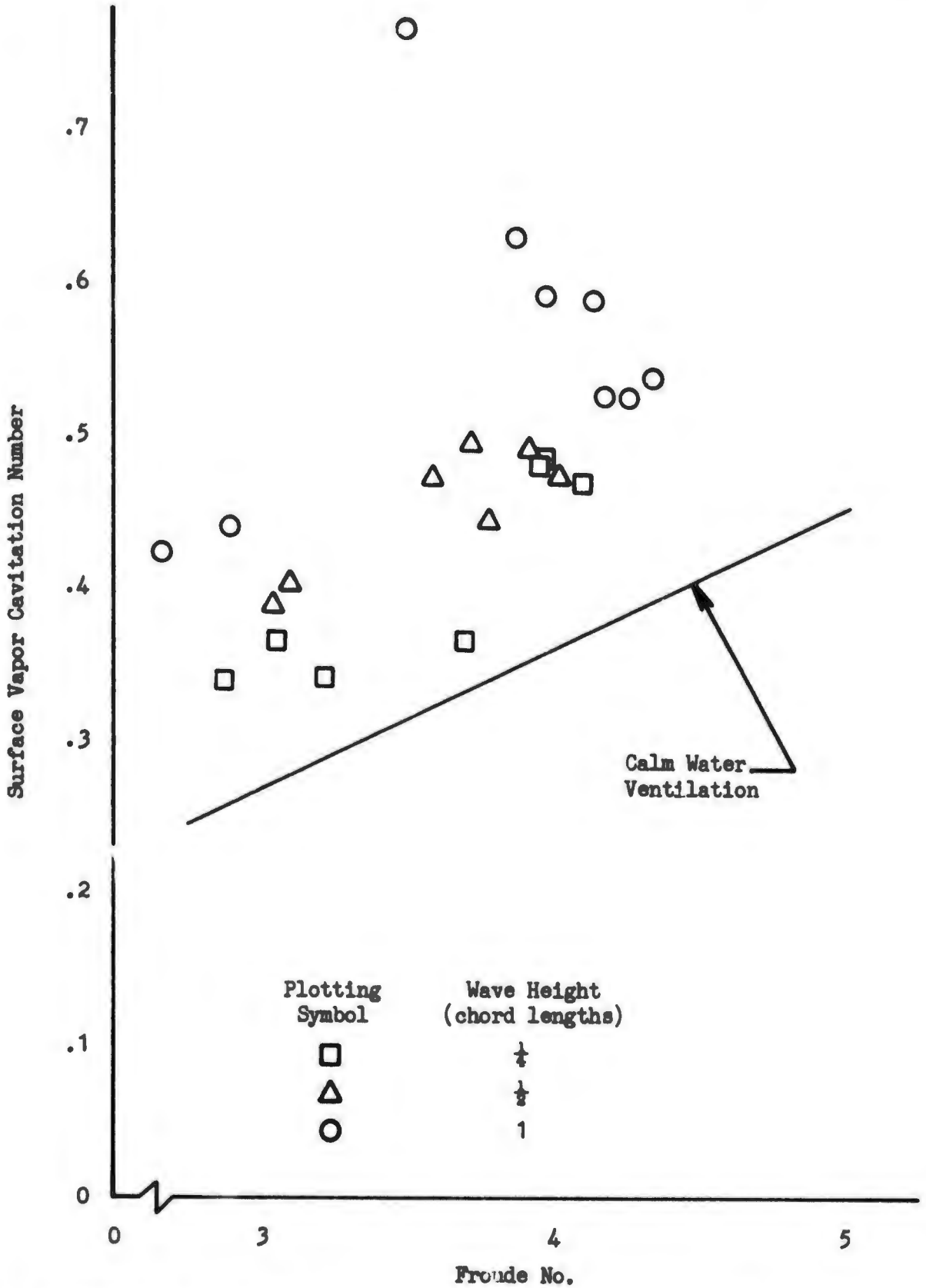

Fig. 9 Effect of head waves on cavitation number at ventilation inception. Strut model 2, blunt-based, 0.76 foot chord, at 8 degrees yaw. 1 chord submergence. Wave length, 14 chords.

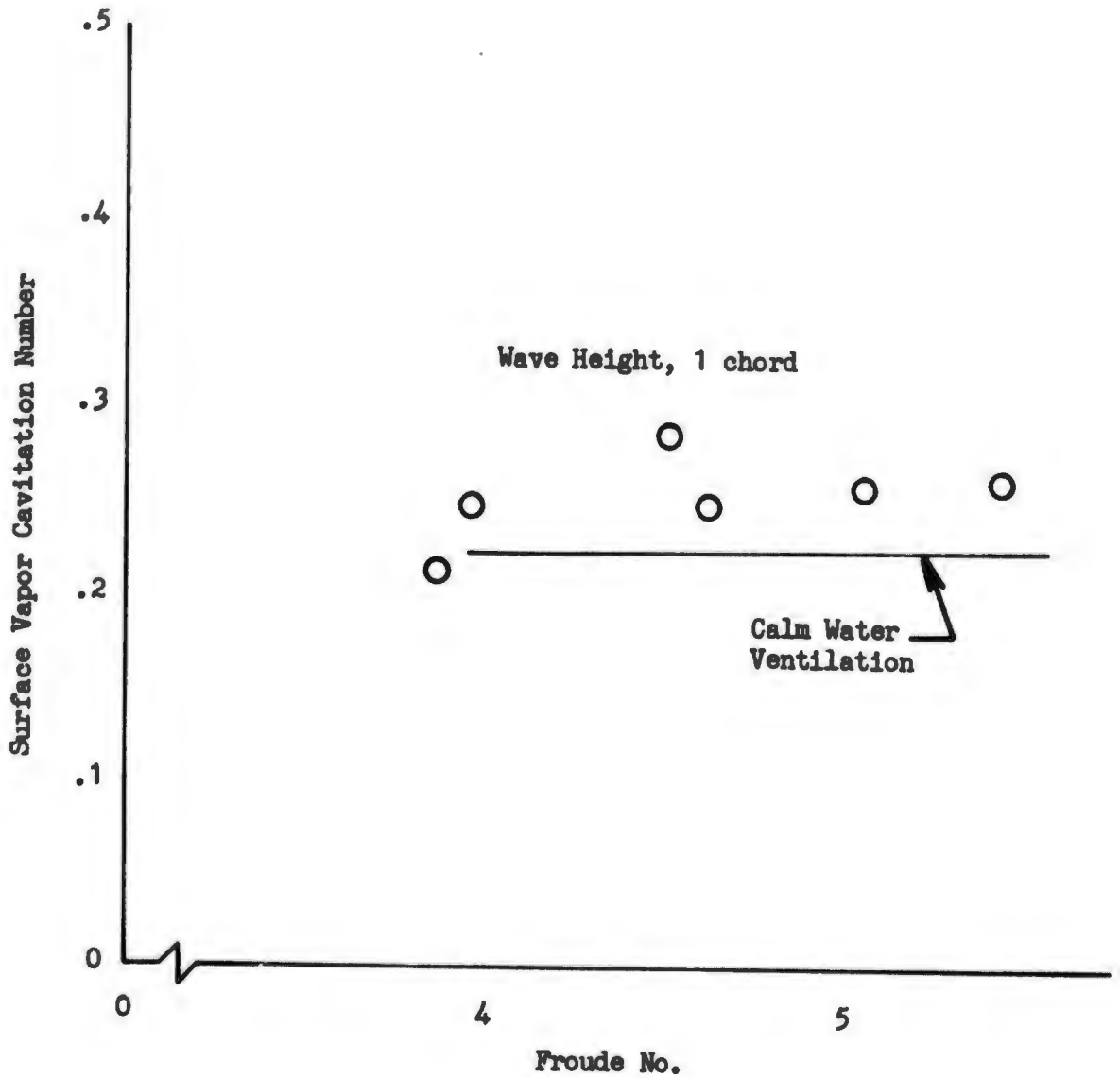

Fig. 10 Effect of head waves on cavitation number at ventilation inception. Strut model 2, blunt-based, 0.50 foot chord, at 6 degrees yaw. 1 chord submergence. Wave length, 14 chords.

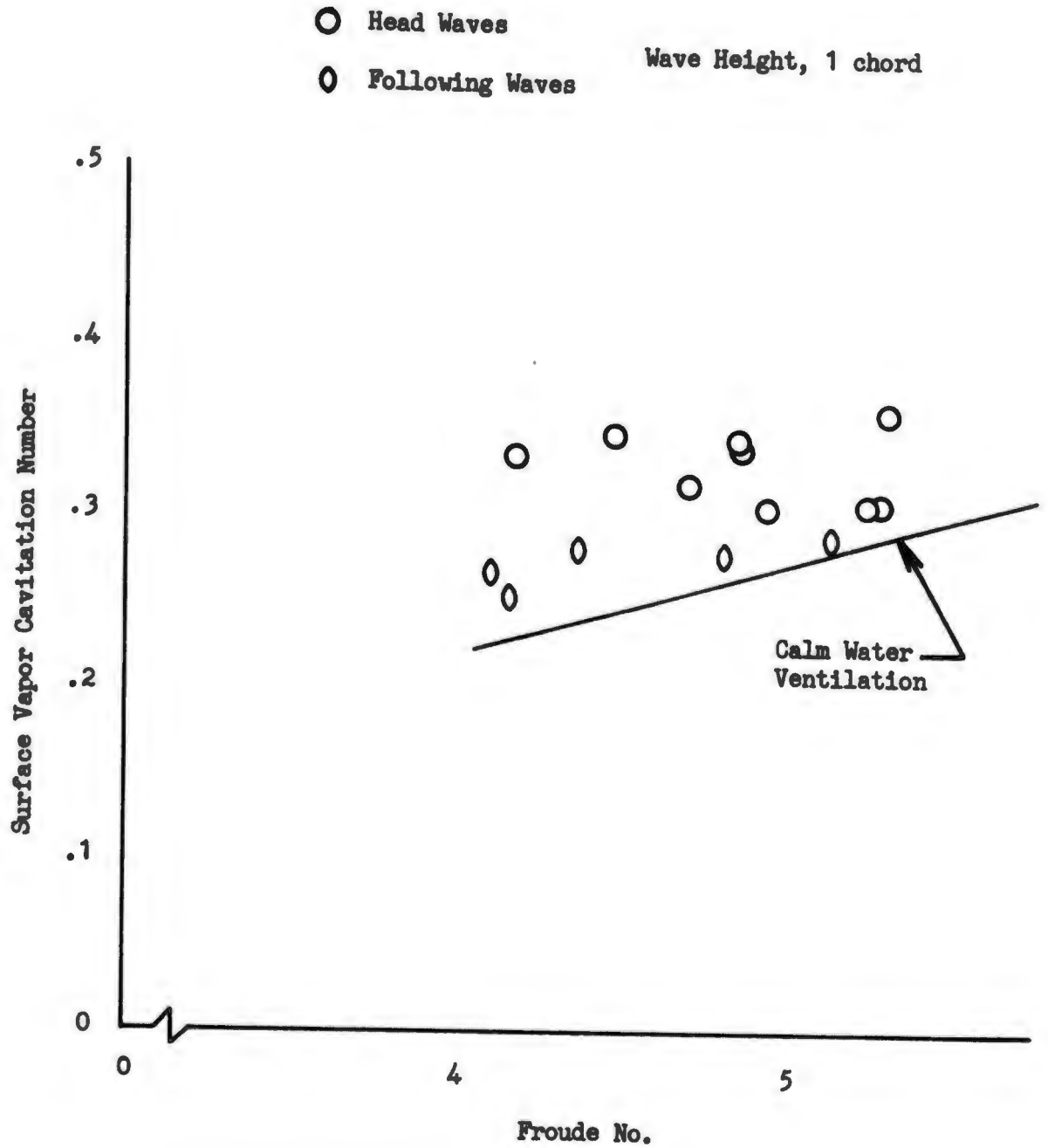

Fig. 11 Effect of head and following waves on cavitation number at ventilation inception. Strut model 2, blunt-based, 0.50 foot chord, at 8 degrees yaw. 1 chord submergence. Wave length, 14 chords.

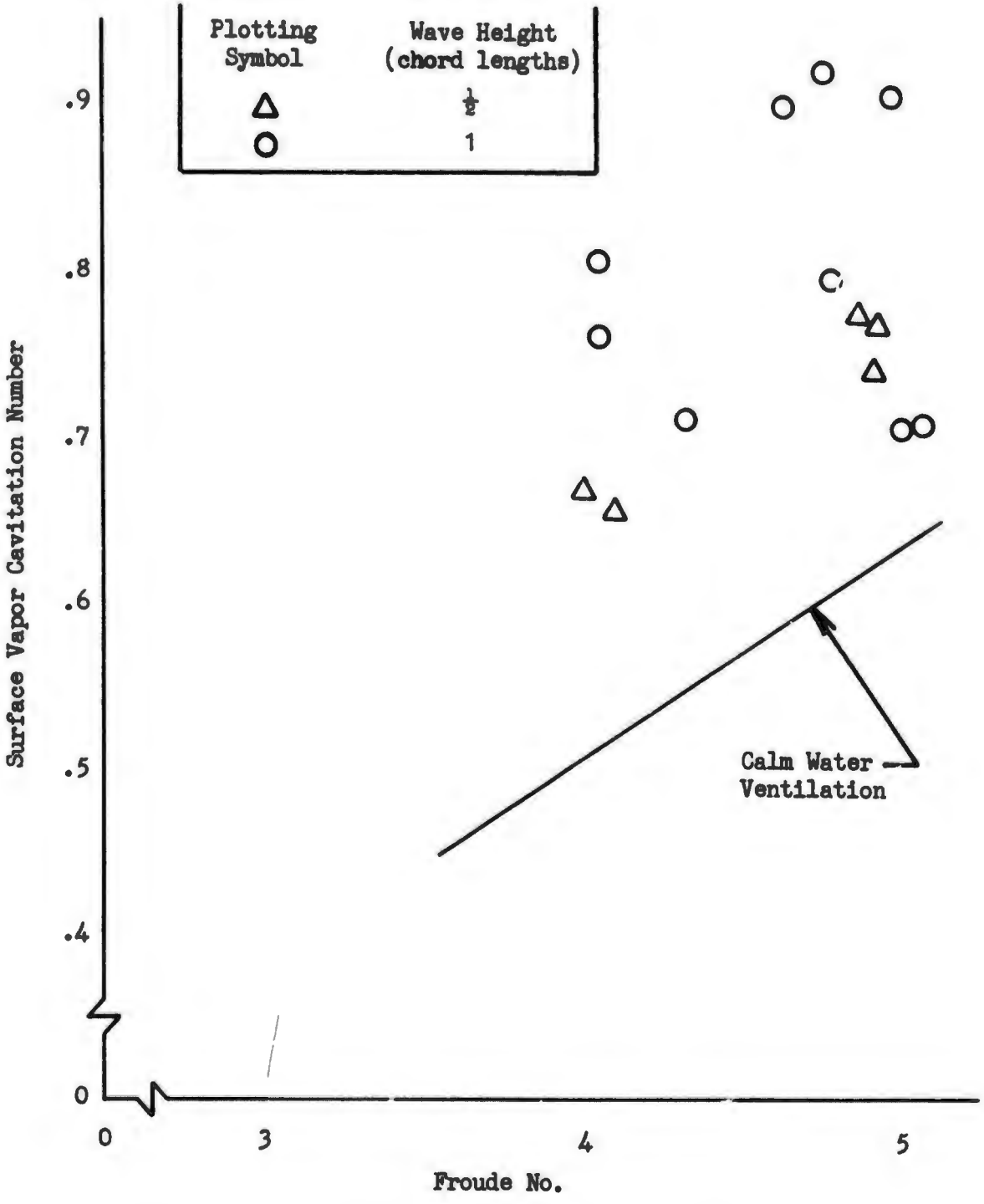

Fig. 12 Effect of head waves on cavitation number at ventilation inception. Strut model 0, blunt-based, 0.50 foot chord, at 8 degrees yaw. 1 chord submergence. Wave length, 14 chords.

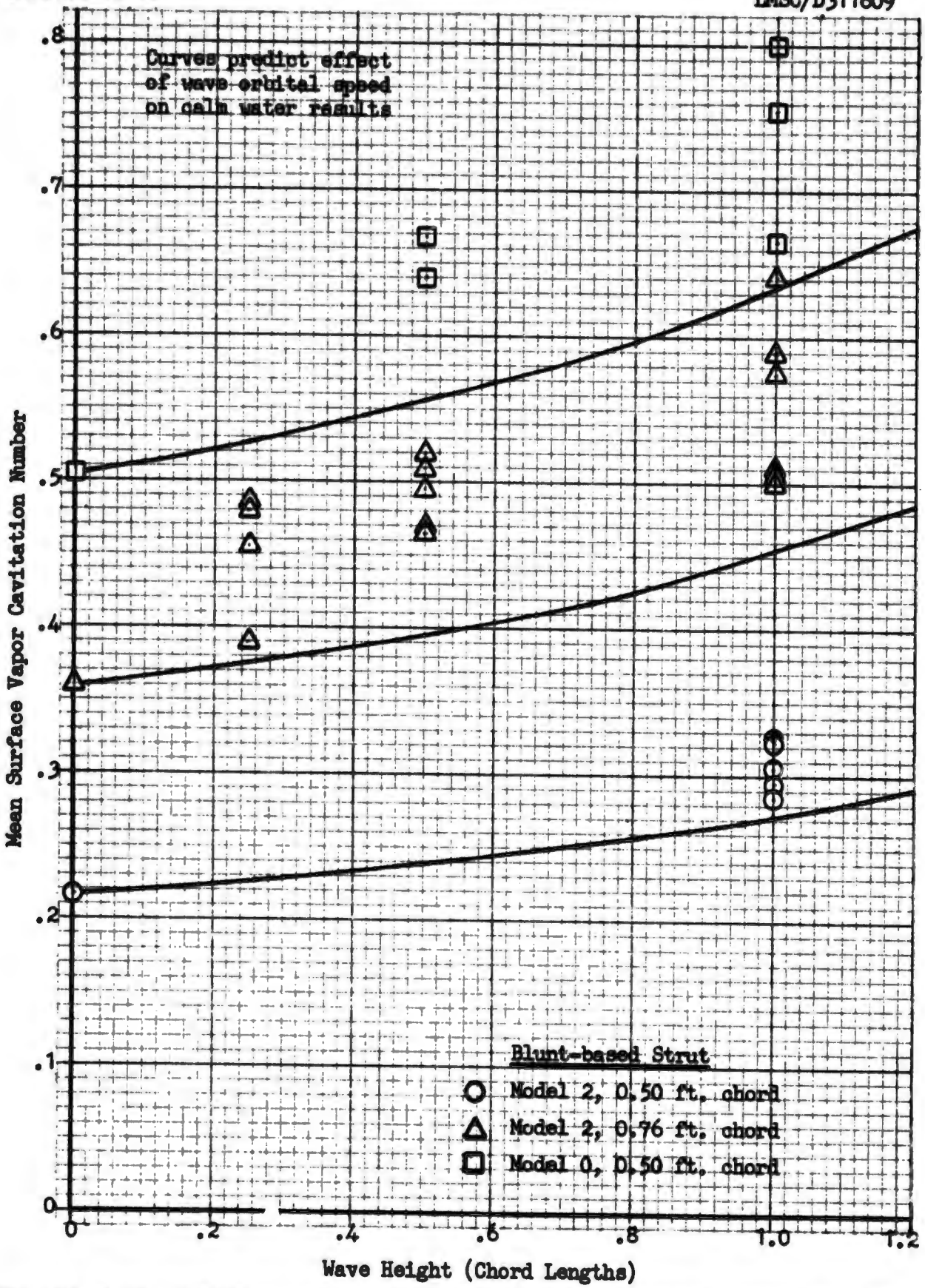

Fig. 13 Mean cavitation number at ventilation inception as a function of wave height. Head waves, 14 chord wave length. Struts at 8 degrees yaw. Froude number 4.

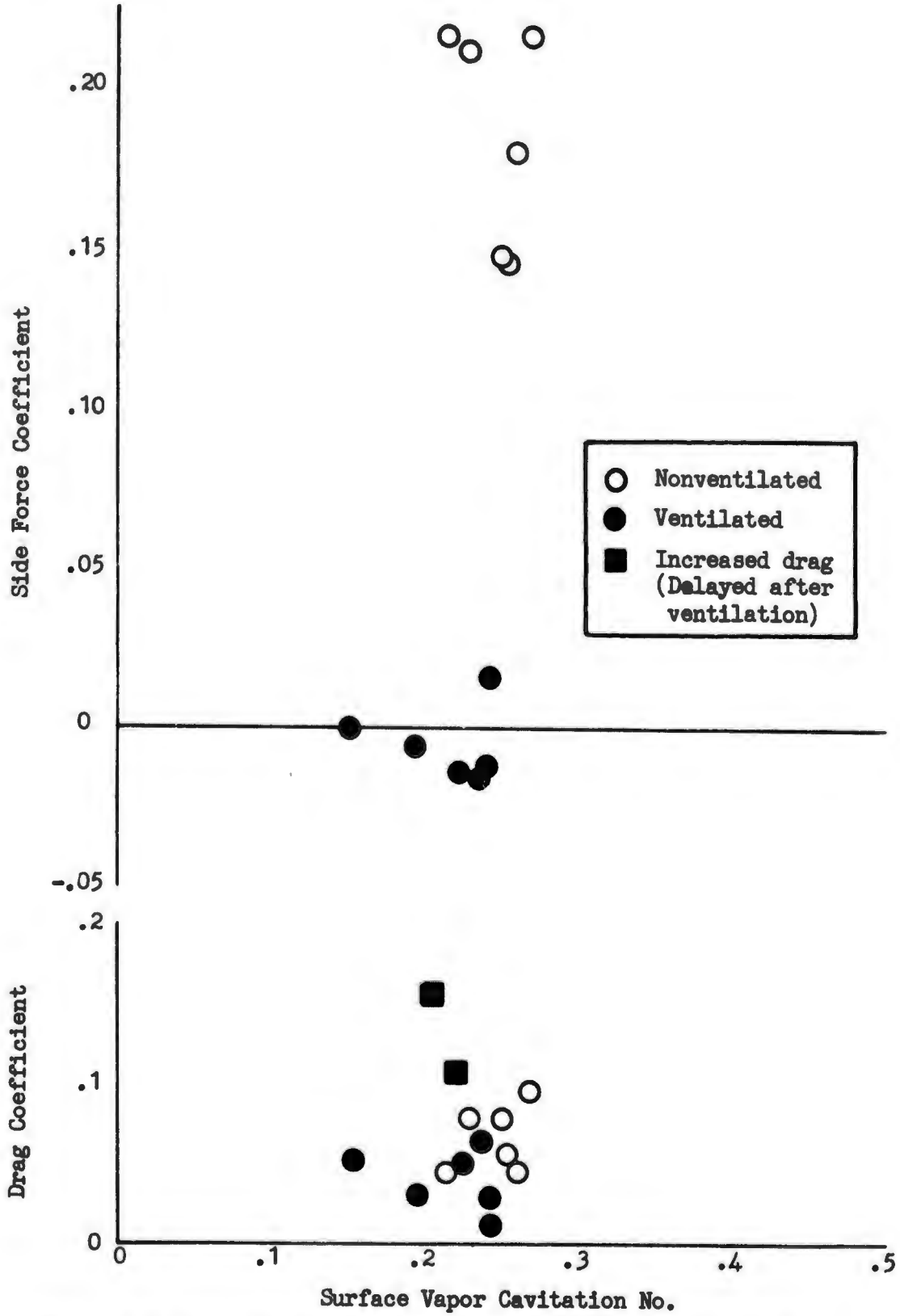

Fig. 14 Side force and drag coefficients for blunt-based strut model 2, 0.76 foot chord, at 6 degrees yaw. Submergence 1 chord length.

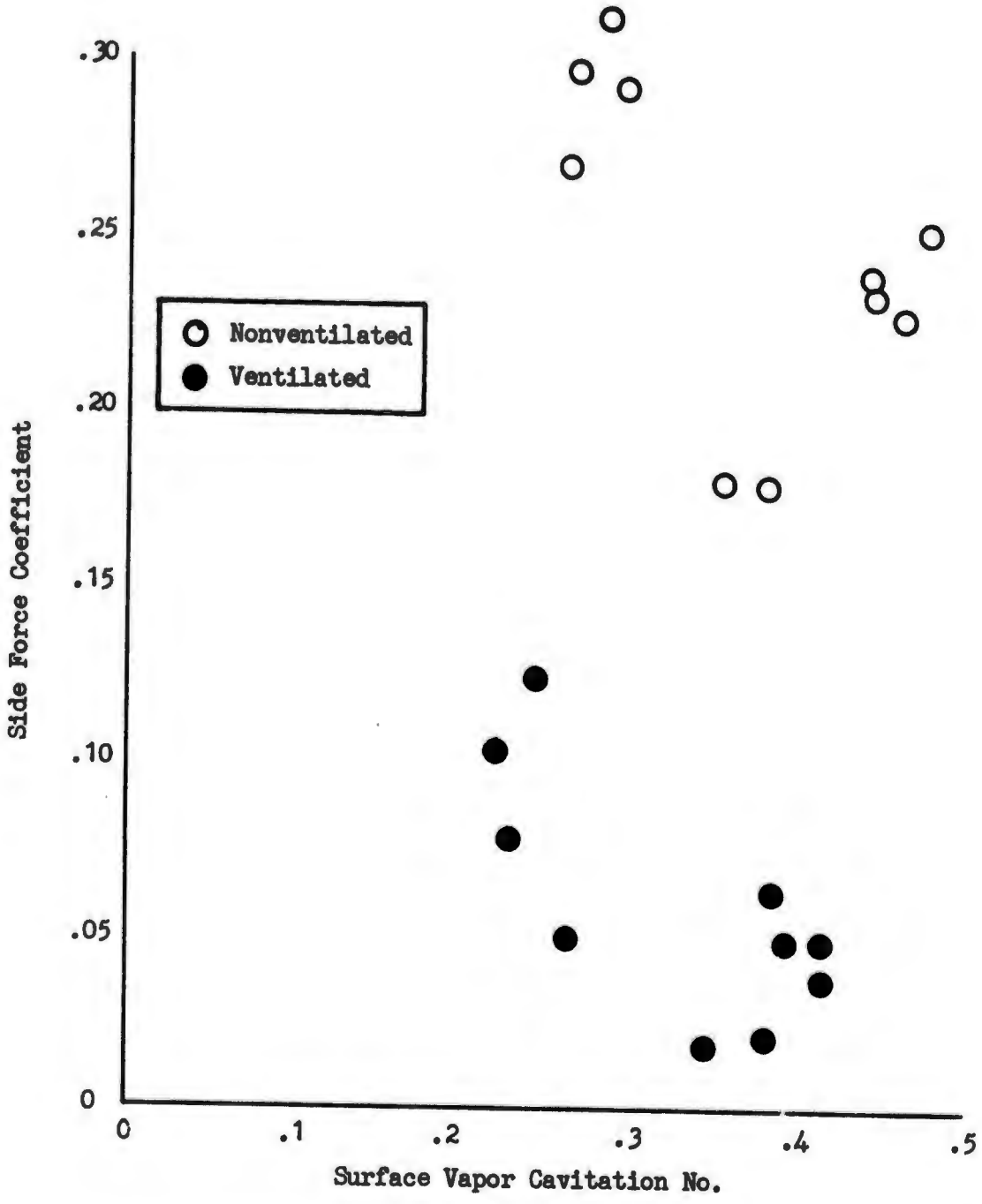

Fig. 15 Side force coefficient for blunt-based strut model 2, 0.76 foot chord, at 8 degrees yaw. Submergence 1 chord length.

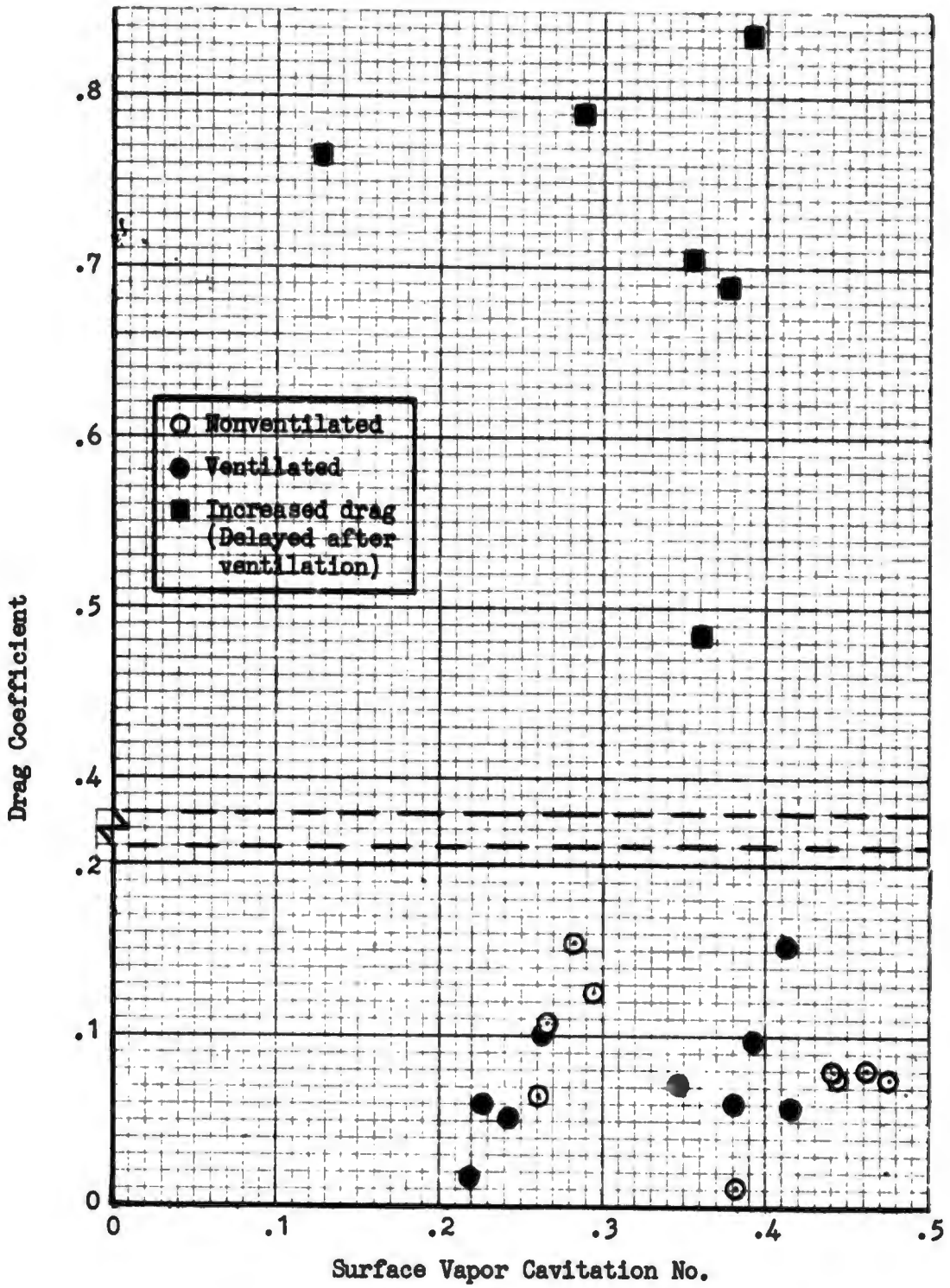

Fig. 16 Drag coefficient for blunt-based strut model 2, 0.76 foot chord, at 8 degrees yaw, Submergence 1 chord.

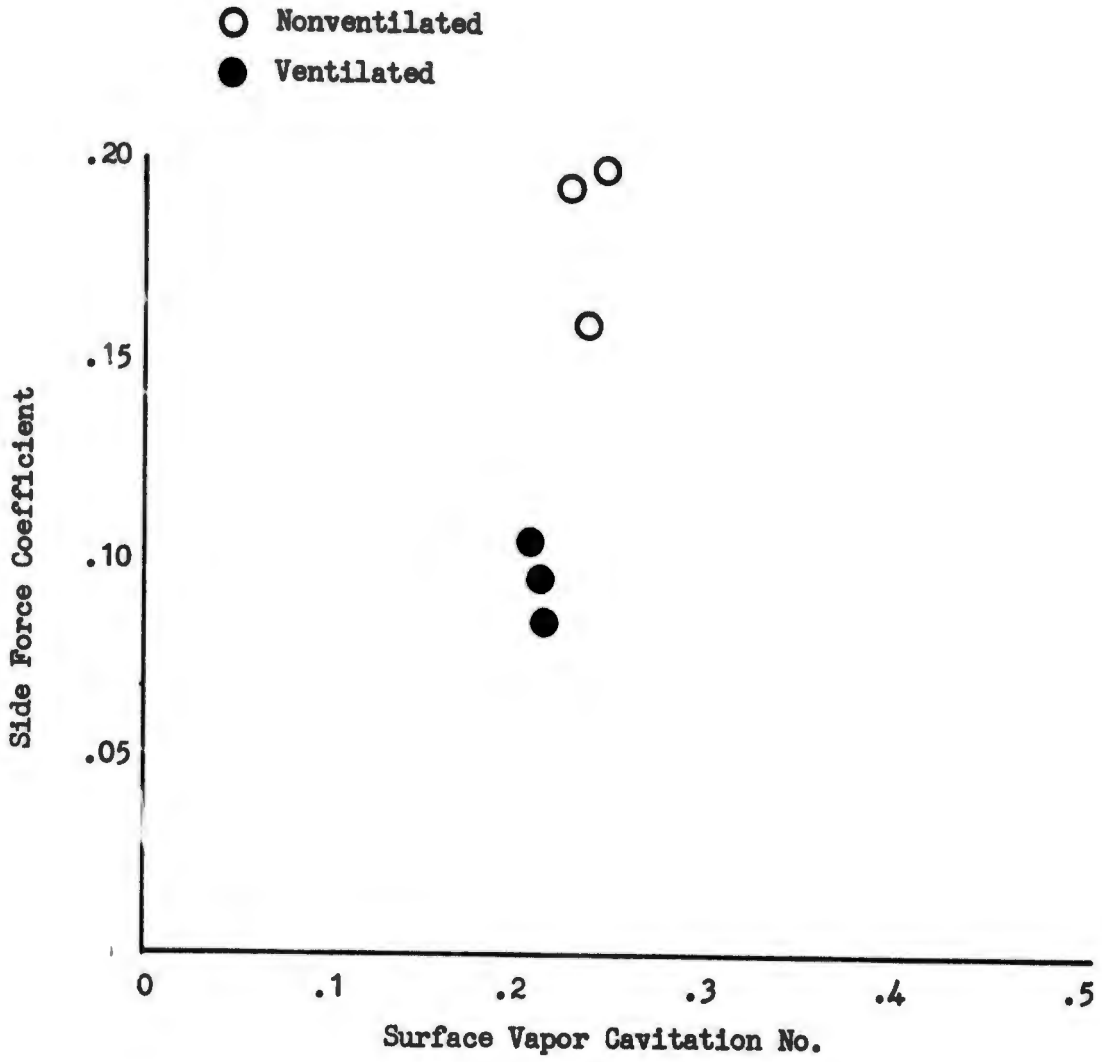

Fig. 17 Side force coefficient for blunt-based strut model 2, 0.50 foot chord, at 6 degrees yaw. Submergence 1 chord.

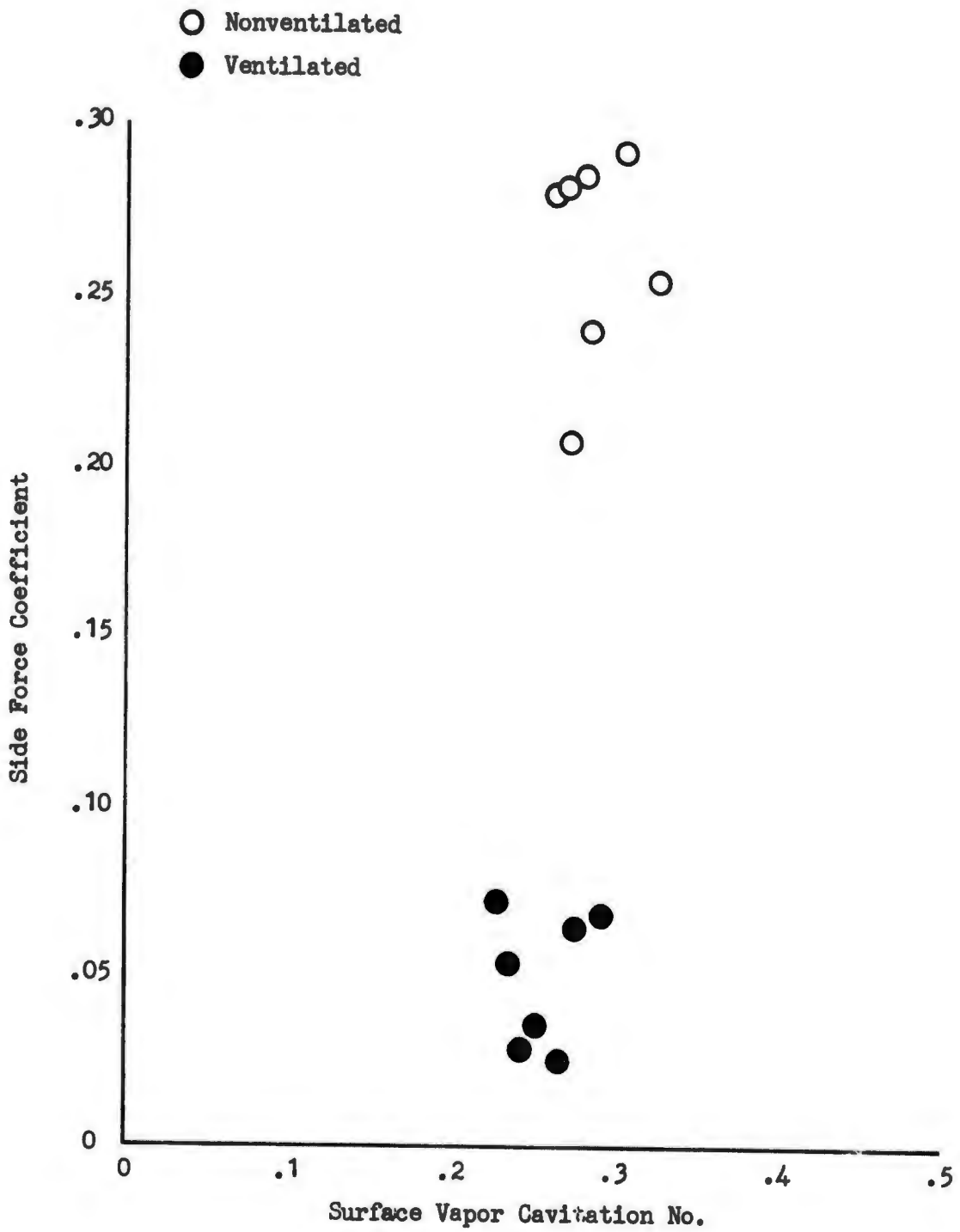

Fig. 18 Side force coefficient for blunt-based strut model 2, 0.50 foot chord, at 8 degrees yaw. Submergence 1 chord.

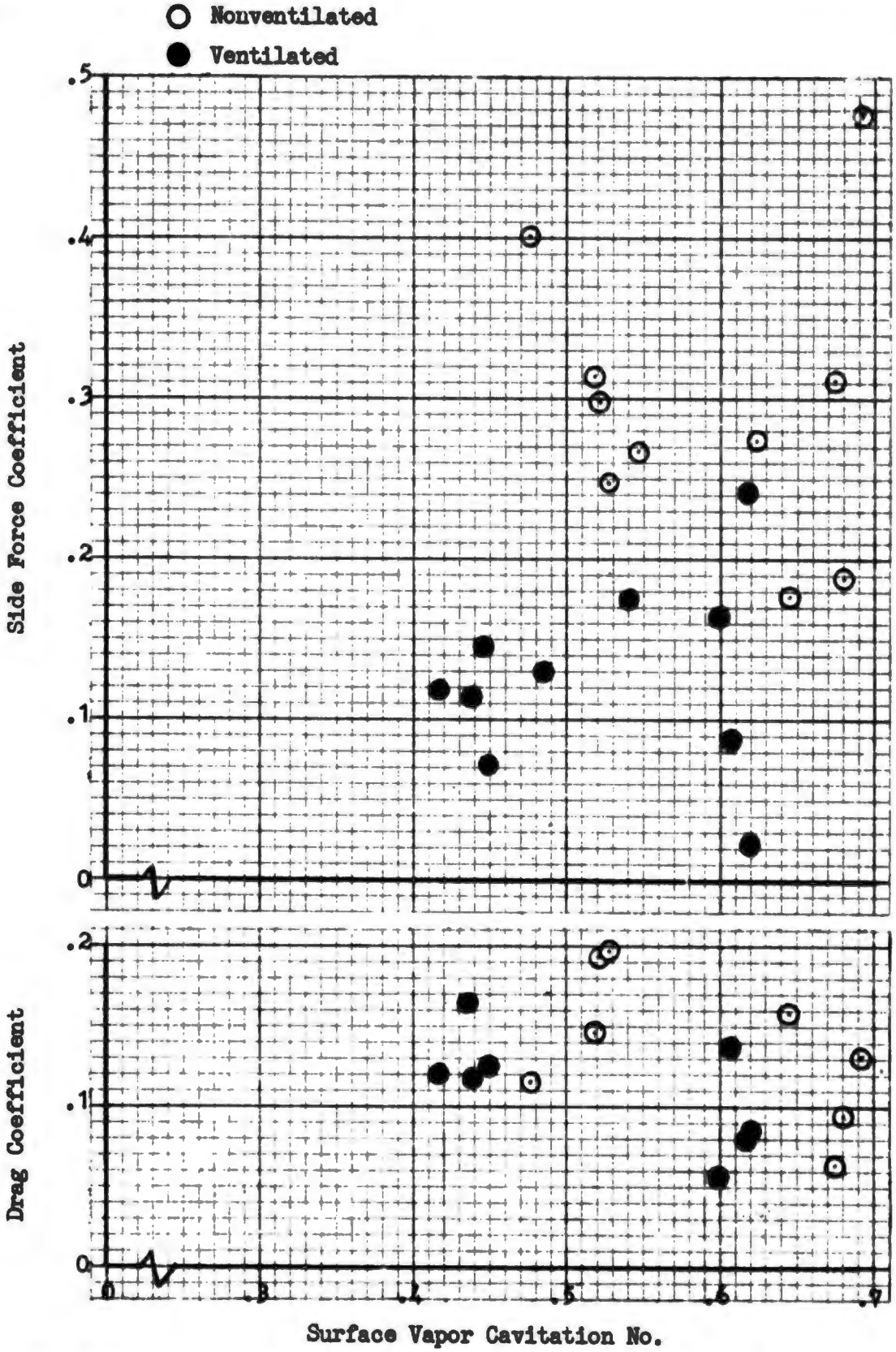

Fig. 19 Side force and drag coefficient for blunt-based strut model 0, 0.50 foot chord, at 8 degrees yaw. Submergence 1 chord.

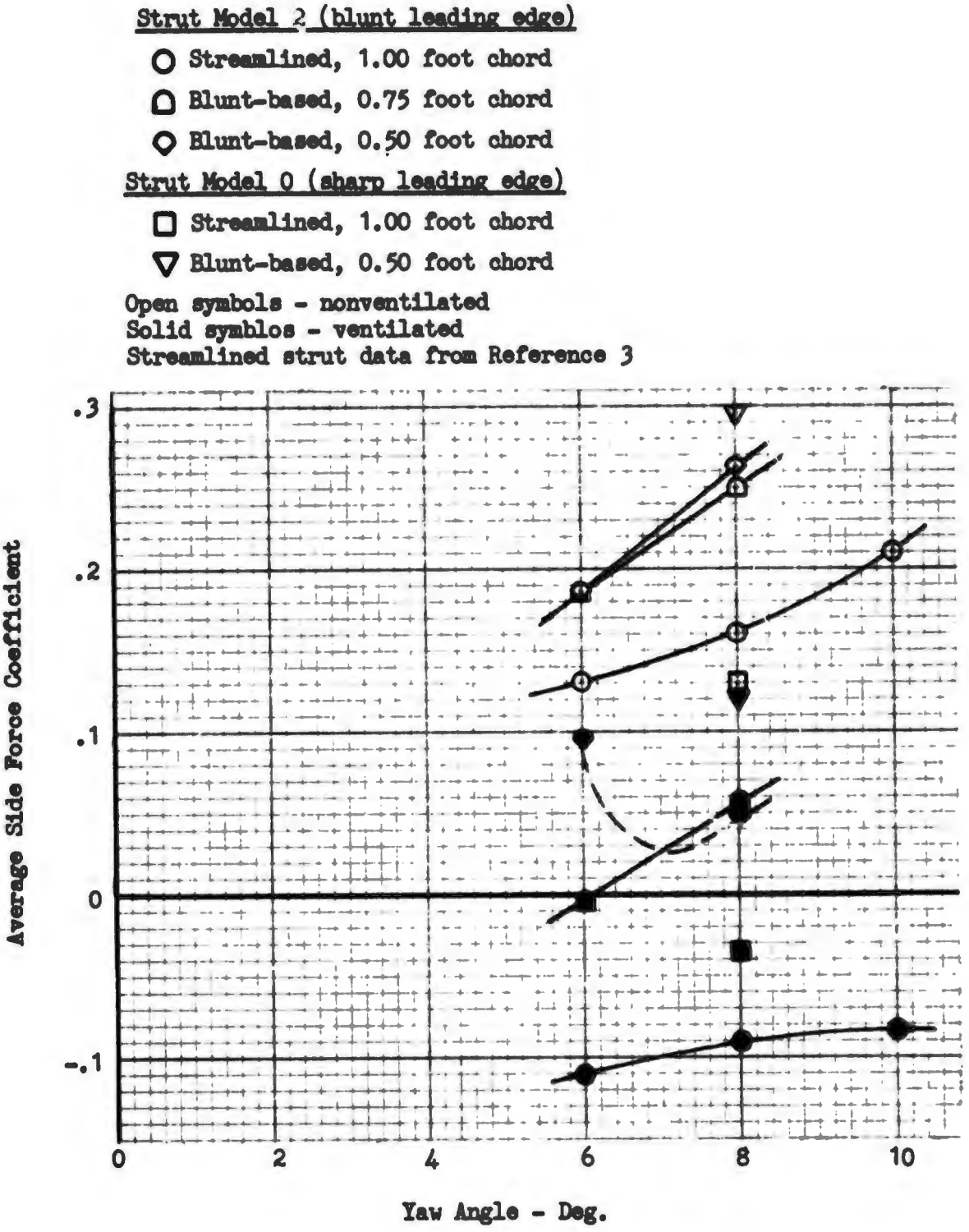

Fig. 20 Average side force coefficient comparison for blunt-based and streamlined struts, each with sharp and blunt leading edges.

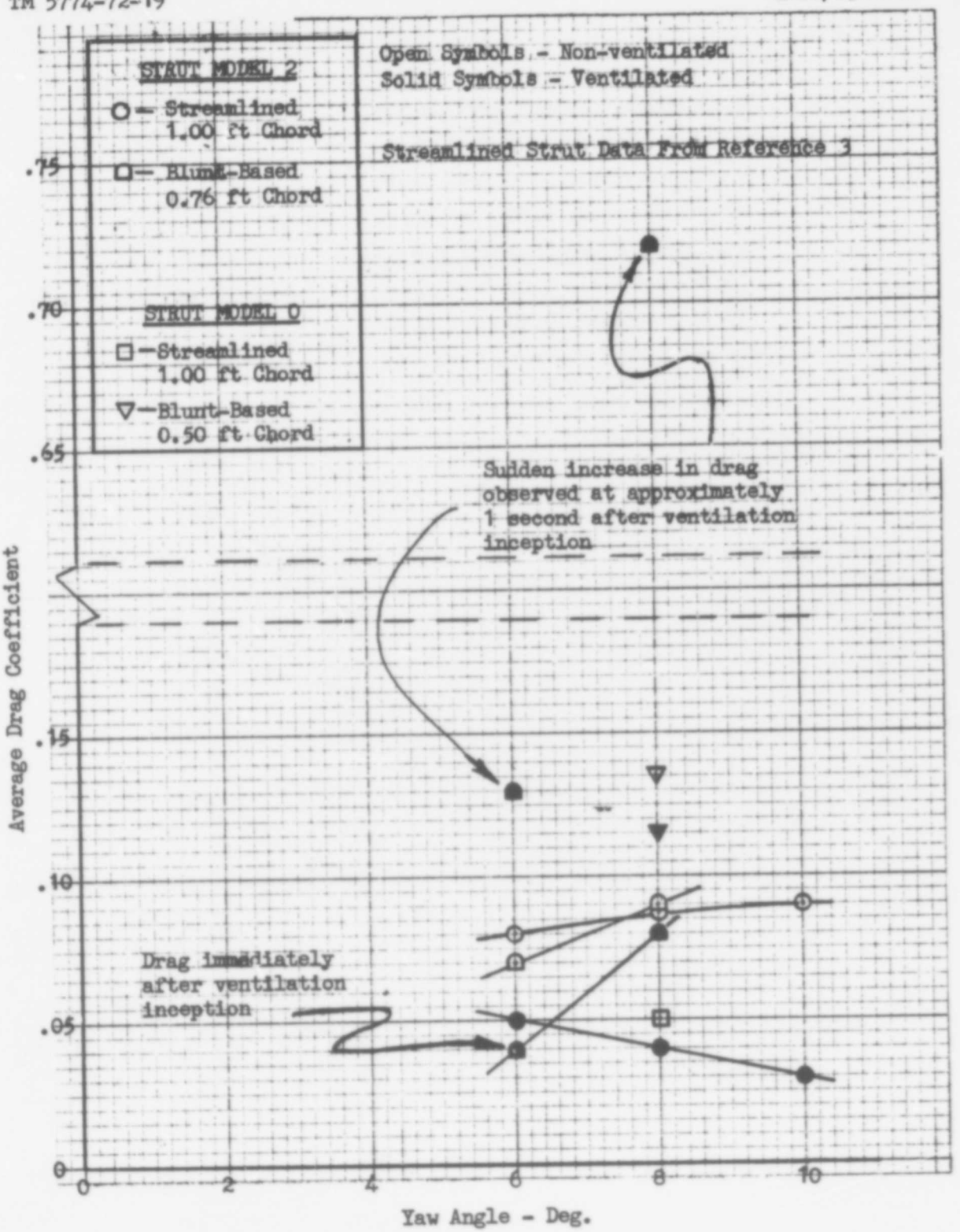

Fig. 21 Average drag coefficient comparison for blunt-based and streamlined struts, each with sharp and blunt leading edges.